Network Modeling Analysis in Health Informatics and Bioinformatics (2024) 13:28
https://doi.org/10.1007/s13721-024-00465-2

ORIGINAL ARTICLE

# Mathematical model of mixed invasive ductal and lobular breast cancer

**Himanshu Jain**[1] · **Arvind Kumar Sinha**[1]

Received: 12 February 2024 / Revised: 4 May 2024 / Accepted: 7 May 2024 / Published online: 22 May 2024


## Abstract

Mixed invasive ductal and lobular carcinoma (Mi-DLC) is a subtype of breast cancer having both ductal and lobular morphology. The coexistence of both morphologies together is not sufficiently addressed in earlier research, so the metastatic behavior of Mi-DLC is not known to healthcare professionals. We introduce the mathematical model to analyze the metastatic behavior of Mi-DLC for controlling the proliferation of tumors. Breast cancer is highly sensitive to estrogen receptors. We incorporate estrogen in the competition among the population of healthy cells, lobular cells, ductal cells, and immune cells. The ketogenic diet sensitizes cancer cells and alters their metabolism. We obtain the increase in the ketogenic diet with the use of anticancer drugs in humans, resulting in a stable cancer-free equilibrium state. We find that the immune response of humans is incapable of fighting the disease when the initial volume of Mi-DLC is high and the ketogenic diet rate is low in the body. The model has four cancer invasion equilibriums: lobular cancer invasion, ductal cancer invasion, mixed ductal and lobular invasion, and dead equilibrium state. We obtain all four cancer invasion equilibriums are stable when we consider the low rate of the ketogenic diet in the body. We calculate that with the proper use of anticancer drugs and a ketogenic diet in humans, the Mi-DLC moves to its dormant stage, and the co-existing equilibrium is stable. The numerical simulation supports the mathematical analysis of the model and establish that the 10% increase in ketogenic diet rate leads to the inhibition of both lobular and ductal tumor cells by 60% and 70%, respectively. The model represents the ketogenic diet with all the other therapies together as the promising adjuvant to inhibit the growth of tumors. The model is helpful in finding the metastatic behavior of Mi-DLC to control the proliferation of tumor cells effectively.

**Keywords** Breast cancer · Mathematical modeling · Estrogen · Immune booster · Ketogenic diet

## 1 Introduction

Breast cancer (BC) is the most prevalent disease in women worldwide. In 2020, it has replaced lung cancer to become the primary cause of cancer in world. There were approximately 2.3 million new cases of breast cancer, which accounts 11.7% of all cancer cases (Sung et al. 2020). Breast cancer accounts for 685,000 deaths globally in 2020 (World Health Organisation 2023). Epidemiological studies have shown that the global burden of death due to BC is expected to cross almost 2 million by the year 2030 (DeSantis et al. 2011). Breast cancer is the most dangerous public health problem, and we require more strategies to significantly improve the effectiveness of traditional anticancer treatments across various cancer types and forms (Weber et al. 2020; Siegel et al. 2018). Breast cancer is the most common invasive cancer in females worldwide. There are primarily two histological subtypes of breast cancer, namely invasive ductal carcinoma (IDC) and invasive lobular carcinoma (ILC) (Oke et al. 2018). Ductal carcinoma occurs in the inner lining of the milk ducts and has the potential to either stay contained to the ducts as a benign cancer, or to spread outside the ducts as invasive ductal carcinoma. In invasive ductal carcinoma (IDC), cancer cells penetrate the duct wall and proliferate among the adjacent lobules of the breast tissues (Arpino et al. 2004). Lobular carcinoma originates in the lobules of the mammary gland, which are responsible for the production of breast milk. If it extends outside the lobules, it is classified as invasive lobular carcinoma (ILC). Both ILC and IDC have the ability to metastasize and spreading into other organs of the body (Wolff

✉ Arvind Kumar Sinha
aksinha.maths@nitrr.ac.in

[1] Department of Mathematics, National Institute of Technology Raipur, Raipur 492010, Chhattisgarh, India

et al. 2013). Invasive ductal carcinoma (IDC) typically transforms the granular composition of breast tissue and likes to develop a mass. On the other hand, invasive lobular carcinoma (ILC) typically grows in a linear pattern through the adipose tissue of the breast. In terms of global prevalence, IDC is the predominant form of breast cancer, while ILC represents around 10–15% of all breast cancer cases (Metzger-Filho et al. 2019). Figure 1 depicts the anatomical features of ductal and lobular cancer in the human breast. Mixed invasive ductal and lobular carcinoma (Mi-DLC) is a type of breast cancer that is not thoroughly understood. It is characterized by the presence of both ductal and lobular morphology. This category is defined as tumors in which at least 50% of the tumor has a lobular tumor pattern and 10–49% of the tumor has a ductal tumor pattern (Metzger-Filho et al. 2019). Mi-DLC represents around 3–5% of all breast cancer cases (Li et al. 2005). This entity is distinguished by the presence of both ductal and lobular components within a single tumor. European studies have shown a rising trend in the occurrence of Mi-DLC breast cancer from 1987 to 1999. Bharat et al., reported an incidence rate of 6% in the United States. Sastre-Garau et al. (1996) conducted an extensive investigation on breast cancer. A total of 11,036 breast cancer patients who did not have metastasis were analyzed. These patients were treated at the Institut Curie between 1981 and 1991 and their information was systematically recorded in the Breast Cancer database. Out of the total number of patients, 249 were diagnosed with mixed invasive ductal and lobular carcinoma, whereas 726 individuals were associated with invasive lobular carcinoma (ILC), encompassing both its classical form and its histological variants (Sastre-Garau et al. 1996). The diagnosis of mixed invasive ductal carcinoma with lobular features (Mi-DLC) can be complex as it needs thorough inspection by pathologist to discern the presence of both ductal and lobular characteristics inside the tumor. This diagnosis may need the use of specific diagnosis techniques.

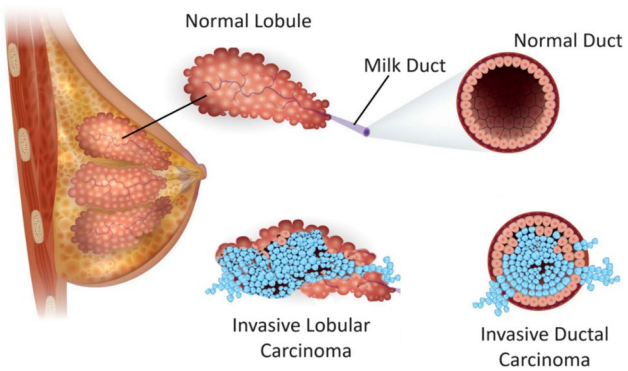


**Fig. 1** The visual representation of ILC and IDC in breast anatomy

Breast cancers are very responsive to natural female hormones, particularly estrogen and progesterone (Mayo Clinic 2023). Breast cancer cells have receptors on their exterior wall which can selectively bind to particular hormones present in the bloodstream (Wolff et al. 2013). Approximately 70% of breast cancers are classified as ER-positive, and a significant number of these patients experience successful eradication of their illness. However, the implementation of efficient hormonal and targeted treatments, 50% of these individuals will experience a recurrence or progress to an untreatable metastatic condition (Harper et al. 2018). The sensitivity of breast cancer to estrogen hormones provides doctors and healthcare professionals with valuable insights for both treating the disease and preventing its recurrence. There are ample number of evidence to support the fact that a ketogenic diet may be beneficial in the treatment of certain forms of cancer (Weber et al. 2020). The concept of ketogenic diet was initially developed in 1921 by Dr. Russel Wilder for the management of refractory seizures in pediatric patients (Kim 2017). A ketogenic (keto) diet is a dietary strategy with high intake of fat and a low intake of carbohydrates. It promotes weight loss by compelling your body to metabolize fat instead of carbohydrates as its primary energy source. The ketogenic diet likely produces an unfavorable nutritional environment for cancer cells, making it a suitable adjuvant for patient-specific combinatorial therapy. A ketogenic diet (KD) induces a metabolic transition from glycolysis to mitochondrial metabolism, resulting in a distinct stress resistance phenomenon that enhances tumor control while reducing complications in normal tissues (Klement 2018). Based on numerous preclinical and clinical studies, it is strongly advocated to incorporate the ketogenic diet alongside standard therapies due to its ability to boost the antitumor effects of traditional chemo- and radiotherapy. Furukawa et al. (2018) administered chemotherapy in combination with the modified ketogenic diet for one year in 10 patients with colon cancer and found the ketogenic diet exhibited a response rate of 60% and control of disease by 70% in cancer patient. Nebeling et al. (1995) demonstrated a 21.8% decrease in tumor standardized uptake value. Additionally, the ketogenic diet has demonstrated a high level of safety and tolerability, as well as an improvement in overall quality of life (Kim 2017). The ketogenic diet (KD) presents a promising prospect for addressing these metabolic changes in tumor cells. Recent study indicates that the ketogenic diet (KD) may have the ability to inhibit the growth of tumors, shield healthy cells from harm caused by chemotherapy or radiation, enhance the harmful effects of chemotherapy on cancer cells, and reduce inflammation. In addition, as compared to anticancer medications and conventional therapies, the ketogenic diet (KD) is cost-effective, very simple to adopt

(with various reliable recipes accessible through books and the internet), and generally well-tolerated (Klement and Sweeney 2016; Rieger et al. 2010, 2014).

The anti-cancer medication tamoxifen is categorized as a selective estrogen receptor modulator (SERM). It is used for the treatment of breast cancer in both males and females, and also as a preventive measure against breast cancer in females (Quirke 2017). The medicine was initially synthesized in 1962 with the aim of functioning as a contraceptive, however, it was found to be unsuitable for that purpose. Nevertheless, it has already demonstrated remarkable efficacy as a drug for cancer treatment (Quirke 2017). A significant milestone in the transition of tamoxifen from a neglected treatment to a highly popular medication took place during the 1980s. This was due to the findings of clinical trials which shown its efficacy as an adjuvant to surgery and chemotherapy in the initial phases of the disease (Lee et al. 2008). Tamoxifen exhibits both estrogenic agonist and antagonist effects in various organs of body. It binds to estrogen receptors, causing both estrogenic and antiestrogenic actions. Because of its dual method of action, it is classified as a patient-specific selective estrogen receptor modulator (SERM). Within the breast tissue, it competes antagonistically with estrogen for binding sites, leading to antiestrogenic and anticancer effects. By interfering with subsequent intracellular processes, it has cytostatic properties, hence inhibiting cell division (Lee et al. 2008). The mathematical models can analyze the interactions between tumor angiogenesis and the metabolic changes induced by a ketogenic diet. This understanding can be valuable for identifying potential targets for intervention. Over the years, modeling breast cancer becomes a valuable tool to understand the dynamical behavior of tumor growth in the treatment process. Mathematical models can provide predictive tools that help researchers and healthcare professionals understand the behavior of Mi-DLC. These models can help estimate the growth, progression, and potential response to treatments of this particular cancer type. Mi-DLC is known for its histological heterogeneity. Mathematical models can help elucidate the underlying biology and behavior of these tumors, providing insights into the different components within the tumor.

Studies in Knútsdóttir et al. (2014); Mirzaei et al. 2021; Yousef et al. 2020a) have shown that mathematical modeling is useful in breast cancer dynamics to better understand the disease spread and to control the tumor proliferation. Mathematical models of immune response to tumor invasion were also developed using population competition models. In 2001, De Pillis and Radunskaya (2001) presented a competition model of four-population that includes tumor cells, host cells, immune cells, and drug interaction. The cancerous tumor growth that includes both the immune system response and drug therapy has been presented by De Pillis and Radunskaya (2001). Tumor cells population, CD8 + T cell population, and Natural Killer cell population competed in a way almost similar to that suggested by Lotka–Volterra's competition models given by De Pillis and Radunskaya (2003). This carries a fundamental aspect on the interaction between immune cells and tumor cells. Mufudza et al. (2012) presented four-population model that includes tumor cells, host cells, immune cells, and estrogen. The effects of estrogen are then incorporated in the model. The results show that the presence of extra estrogen increases the risk of developing breast cancer. Oke et al. (2018) improved the model of Mufudza et al. (2012) in 2018. They incorporated control parameters such as ketogenic diet, immune booster, and anticancer drug under the assumption that there is an interaction between healthy cells and lobular carcinoma cells. In 2023, Nasrazadani et al., observed the higher concordance in clinicopathologic characteristics between Mi-DLC and invasive lobular carcinoma. The characteristics of Mi-DLC growth dynamics has dominance of lobular pathology. The coexistence of both morphologies together is not sufficiently addressed in earlier research, so the metastatic behavior of Mi-DLC is not known to healthcare professionals. However, these studies did not explore about the effect of any control parameters in the dynamic behavior of mixed invasive ductal and lobular type of breast cancer.

The objective of this study is to develop a mathematical model that represents the growth and progression dynamics of Mi-DLC to assess the effect of ketogenic diet with drug therapy. We use differential equation for each population of healthy cells, lobular tumor cells, ductal tumor cells, immune cells, and estrogen. The model has the potential to help healthcare professionals to obtain more treatment strategy, provide insights into tumor growth patterns, and contribute to personalized treatment strategies for patients with Mi-DLC.

After presenting the research objectives, this paper is organized into the following sections to comprehensively address the mathematical modeling of mixed invasive ductal and lobular carcinoma (Mi-DLC). Section 2 contains the formation of a deterministic mathematical model. All the equilibrium points and their stability are shown in Sect. 3. The numerical simulation of the model is demonstrated and explained in Sect. 4. Sections 5 and 6 contains the discussion and conclusion respectively.

## 2 Mathematical model

In this section, the formation of mathematical model is described. The objective is to generate a deterministic mathematical model to show the dynamics of mixed invasive ductal and lobular type of breast cancer. The assumptions are made on the basis of previous mathematical models of

breast cancer dynamics. A mathematical model of immune response to tumor invasion was also developed using competition models. The formation of our proposed model is based on model given by Mufudza et al. (2012). They presented the mathematical model which incorporates the effects of estrogen on interaction between immune cells and breast cancer cell interaction. We developed a model by assuming the logistic growth of a cell population and basic competition of lobular and ductal cancer cell population to the healthy cell population simultaneously. Considering the case of MiDLC, we have taken breast cancer population as both cell population of invasive ductal carcinoma and invasive lobular carcinoma. We considered the immune cells compartment to comprise Natural Killer cells (NK) and CD8+ T-cells as in De Pillis and Radunskaya (2001). The similar equation to model the immune response dynamic by introducing new parameter of immune booster (ketone bodies) and anticancer drug efficacy is used. We introduce the ketogenic diet to the patient with diet rate $d$, we assume that the ketogenic diet rate alters the carrying capacity of both lobular and ductal cancer cells. We assume that the ketogenic diet produces more ketones in the body, which results in increment of immune response to the tumor proliferation. The effect of tamoxifen drug on breast cancer is applied to the model according to estrogen receptor status. We assume that the majority of lobular and ductal cancer cells are ESR1 $+ve$, which can only be blocked by anticancer drug tamoxifen with efficacy of $(1-k)$. Finally, we result in the following set of equation containing cell population of healthy cells, lobular tumor cells, ductal tumor cells, immune cells, and estrogen.

$$\begin{cases} \frac{dH}{dt} = r_1 H\left(C_1 - a_1 H - b_1 T_L - b_2 T_D\right) - (1-k)\phi_1 HE, \\ \frac{dT_L}{dt} = r_2 T_L\left(C_2 d - a_2 T_L - b_3 I\right) - \delta T_L + \varepsilon(1-k)\phi_1 HET_L, \\ \frac{dT_D}{dt} = r_3 T_D\left(C_3 d - a_3 T_D - b_4 I\right) - \delta T_D + (1-\varepsilon)(1-k)\phi_1 HET_D, \\ \frac{dI}{dt} = \lambda\mu + I\left(C_4 - a_4 - b_5 T_L - b_6 T_D\right) - (1-k)\phi_2 IE, \\ \frac{dE}{dt} = \rho(1-k) - b_7 E. \end{cases} \tag{1}$$

Here, $H$ denotes the healthy cell population, $T_L(t)$ and $T_D(t)$ are lobular cell and ductal cell population respectively, $I$ denotes the immune cell population and $E$ stands for estrogen present in the human body. The carrying capacity $C_1$ and $C_2$ of lobular carcinoma and ductal carcinoma respectively are dependent on ketogenic diet rate $d$. The immune booster $\mu$ assist and enhance the immune response to inhibit the proliferation of tumor cells. $(1-k)$ represents the efficacy of anticancer drugs tamoxifen used for treating both lobular and ductal type of breast cancer. The description of all the parameters is described in Table 1. Here $r_1$ is the growth rat of healthy cell and $a_1$ is the logistic rate of healthy cells. $r_2$ and $r_3$ are the growth rate of lobular and ductal cancer cell, respectively. The source rate of estrogen in patients is taken as $\rho$ whereas $b_7$ is death rate of estrogen to maintain its level in human body. As excess estrogen result in the induced obesity and leads to proliferation of tumor by the rate of $\phi_1$. We have incorporated $(1-k)$ for the positive effect of anticancer drugs on lobular and ductal cancer cells.

## 3 The equilibrium points

The model admits five equilibrium points namely: (i) Cancer-free equilibrium state, (ii) Lobular cancer invasion equilibrium, (ii) Ductal cancer invasion equilibrium, (iii) Mixed ductal and lobular carcinoma invasion equilibrium, (v) Coexisting equilibrium.

### 3.1 Cancer-free equilibrium point

In this subsection, we determine the local behavior of system (1) in the absence of both lobular and ductal tumor cell population. The cancer-free equilibrium point is denoted by $\Lambda_0 = (H_0^*, 0, 0, I_0^*, E_0^*)$, which is obtained by the following subsystem:

$$\begin{cases} 0 = r_1 H\left(C_1 - a_1 H\right) - (1-k)\phi_1 HE, \\ 0 = \lambda\mu + I\left(C_4 - a_4\right) - (1-k)\phi_2 IE, \\ 0 = \rho(1-k) - b_7 E. \end{cases} \tag{2}$$

On solving (2), we obtained $\Lambda_0 = (H_0^*, 0, 0, I_0^*, E_0^*)$, where $H_0^* = \frac{b_7 r_1 C_1 - (1-k)^2\phi_1\rho}{b_7 r_1 a_1}$, $I_0^* = \frac{\lambda\mu b_7}{(1-k)^2\phi_2\rho - b_7(C_4 - a_4)}$, and $E_0^* = \frac{(1-k)\rho}{b_7}$.

**Stability of cancer-free equilibrium point**

We analyze the local stability of system (1) around the cancer-free equilibrium point $\Lambda_0$. The Jacobian matrix of cancer-free equilibrium point $\Lambda_0 = (H_0^*, 0, 0, I_0^*, E_0^*)$ is given as:

$$J(\Lambda_0) = \begin{pmatrix} m_{11} & m_{12} & m_{13} & 0 & m_{15} \\ 0 & m_{22} & 0 & 0 & 0 \\ 0 & 0 & m_{33} & 0 & 0 \\ 0 & m_{42} & m_{43} & m_{44} & m_{45} \\ 0 & 0 & 0 & 0 & m_{55} \end{pmatrix},$$

where $m_{11} = r_1 C_1 - 2r_1 a_1 H_0^* - \frac{(1-k)^2\phi_1\rho}{b_7}$, $m_{12} = -r_1 b_1 H_0^*$, $m_{13} = -r_1 b_2 H_0^*$, $m_{15} = -(1-k)\phi_1 H_0^*$, $m_{22} = r_2 C_2 d - r_2 b_3 I_0^* - \delta + \frac{\varepsilon(1-k)^2\rho\phi_1}{b_7} H_0^*$, $m_{33} = r_3 C_3 d - r_3 b_4 I_0^* - \delta + \frac{(1-\varepsilon)(1-k)^2\rho\phi_1}{b_7} H_0^*$, $m_{42} = -b_5 I_0^*$,

**Table 1** Description of parameters

| Parameter | Description | Value range | References |
|---|---|---|---|
| $r_1$ | The growth rate of healthy cell | 0.3 $day^{-1}$ | Yousef et al. (2020a) |
| $C_1$ | Carrying capacity of healthy cell | 1.232 $day^{-1}$ | Yousef et al. (2020a) |
| $a_1$ | Logistic rate of healthy cell | [0.05, 0.2] $day^{-1}$ | Yousef et al. (2020b) |
| $b_1$ | Rate of inhibition of healthy cell due to lobular tumor | $6 \times 10^{-8}$ $day^{-1}$ | Yousef et al. (2020b) |
| $b_2$ | Rate of inhibition of healthy cell due to ductal tumor | $5 \times 10^{-8}$ $day^{-1}$ | Yousef et al. (2020b) |
| $k$ | Efficacy of anti-cancer drug | [0, 1] $day^{-1}$ | Yousef et al. (2020b) |
| $\phi_1$ | Tumor formation rate as a result of DNA damage by excess estrogen | 0.2 $day^{-1}$ | Yousef et al. (2020a) |
| $r_2$ | The growth rate of lobular tumor cell | [0.5, 0.89] $day^{-1}$ | Yousef et al. (2020a) |
| $C_2$ | Carrying capacity of lobular tumor cell | 1.75 $day^{-1}$ | Yousef et al. (2020a) |
| $d$ | Constant rate of the ketogenic diet | [0, 0.7] $day^{-1}$ | Yousef et al. (2020a) |
| $a_2$ | Logistic rate of lobular tumor cell | [0.5, 0.95] $day^{-1}$ | Yousef et al. (2020a) |
| $b_3$ | Ductal tumor cell death rate due to immune response | $3 \times 10^{-6}$ $day^{-1}$ | Yousef et al. (2020b) |
| $\delta$ | The death rate of tumor cell due to the ketogenic diet | [0, 1] $day^{-1}$ | Assumed |
| $\varepsilon$ | Proportion of effectiveness of anticancer drug on lobular tumor cell | 0.3 $day^{-1}$ | Assumed |
| $r_3$ | The growth rate of ductal tumor cell | 0.4 $day^{-1}$ | Yousef et al. (2020a) |
| $C_3$ | Carrying capacity of ductal tumor cell | 1.75 $day^{-1}$ | Yousef et al. (2020a) |
| $a_3$ | Logistic rate of ductal tumor cell | [0.5, 0.95] $day^{-1}$ | Yousef et al. (2020a) |
| $b_4$ | Ductal tumor cell death rate due to immune response | $3 \times 10^{-6}$ $day^{-1}$ | Yousef et al. (2020b) |
| $\lambda$ | Source rate of immune cell | $1.3 \times 10^{2}$ $day^{-1}$ | Yousef et al. (2020a) |
| $\mu$ | Supplement of immune booster | 0.01 $day^{-1}$ | Yousef et al. (2020a) |
| $C_4$ | Carrying capacity of immune cell | [0.11, 1.17] $day^{-1}$ | Yousef et al. (2020a) |
| $a_4$ | Logistic growth rate of immune cells | [0.05, 0.2] $day^{-1}$ | Yousef et al. (2020b) |
| $b_5$ | Interaction coefficient rate of lobular tumor cell with immune response | $1 \times 10^{-7}$ $day^{-1}$ | Yousef et al. (2020a) |
| $b_6$ | Interaction coefficient rate of ductal tumor cell with immune response | $1 \times 10^{-7}$ $day^{-1}$ | Yousef et al. (2020a) |
| $\phi_2$ | Immune suppression rate due to excess estrogen | 0.002 $day^{-1}$ | Yousef et al. (2020a) |
| $\rho$ | Source rate of estrogen | [0.06, 0.9] $day^{-1}$ | Yousef et al. (2020a) |
| $b_7$ | The natural death rate of estrogen | 0.31 $day^{-1}$ | Yousef et al. (2020a) |

$m_{43} = -b_6 I_0^*, m_{44} = C_4 - a_4 - \frac{(1-k)^2 \rho \phi_2}{b_7}, m_{45} = -(1-k)\phi_2 I_0^*$, $m_{55} = -b_7$.

We have the characteristic equation of $\Lambda_0$ as:

$$(m_{11} - \lambda)(m_{22} - \lambda)(m_{33} - \lambda)(m_{44} - \lambda)(m_{55} - \lambda) = 0 \quad \text{(a)}$$

Thus, the local stability for $\Lambda_0 = (H_0^*, 0, 0, I_0^*, E_0^*)$ is obtained in Theorem 1 as follows.

**Theorem 1** *$\Lambda_0$ is the cancer-free equilibrium point of system (1) and let $\phi_1 > \frac{r_1 C_1 b_7}{\rho(1-k)^2}$ and $\phi_2 > \frac{(C_4-\delta)b_7}{\varepsilon(1-k)^2}$ hold. Then $\Lambda_0$ is stable local asymptotic if and only if $H_0^* < \min\left(\frac{(\delta - r_2 C_2 d)b_7}{(1-k)^2 \phi_1 \rho \varepsilon}, \frac{(\delta - r_3 C_3 d)b_7}{(1-k)^2 \phi_1 \rho (1-\varepsilon)}\right)$, where $r_2 < \frac{\delta}{C_2 d}$ and $r_3 < \frac{\delta}{C_3 d}$.*

***Proof:*** From (a), it follows that

(i) $\lambda_1 = r_1 C_1 - 2 r_1 a_1 H_0^* - \frac{(1-k)^2 \phi_1 \rho}{b_7} < 0, \text{since} \phi_1 > \frac{r_1 C_1 b_7}{\rho(1-k)^2}$.

(ii) $\lambda_2 = r_2 C_2 d - r_2 b_3 I_0^* - \delta + \frac{\varepsilon(1-k)^2 \rho \phi_1}{b_7} H_0^* < 0 \Rightarrow H_0^* < \frac{(\delta - r_2 C_2 d)b_7}{(1-k)^2 \phi_1 \rho \varepsilon}$, where $r_2 < \frac{\delta}{C_2 d}$.

(iii) $\lambda_3 = r_3 C_3 d - r_3 b_4 I - \delta + \frac{(1-\varepsilon)(1-k)^2 \rho \phi_1}{b_7} H_0^* < 0$
$\Rightarrow H_0^* < \frac{(\delta - r_3 C_3 d)b_7}{(1-k)^2 \phi_1 \rho (1-\varepsilon)}$, where $r_3 < \frac{\delta}{C_3 d}$.

(iv) $\lambda_4 = -\frac{[(1-k)^2 \rho \phi_2 - b_7 (C_4 - a_4)]}{b_7} < 0$, since $\phi_2 > \frac{(C_4 - a_4)b_7}{\rho(1-k)^2}$.

(v) $\lambda_5 = -b_7 < 0$.

Theorem 1 indicates that if we increase the ketogenic diet rate, it alters the growth of the Mi-DLC population. If the initial value of the lobular and ductal tumor cells population is low, then increasing the ketogenic diet rate with proper usage of anticancer drug result in elimination of Mi-DLC from breast tissue. We observe that, $\Lambda_0$ depends heavily on the immune cell population and the level of estrogen in the body.

### 3.2 Lobular cancer invasion equilibrium point

When ductal carcinoma cells are low in volume and not able to compete with resources with lobular cancer cells, the lobular cell dominants the cell population and remains in the body. In this subsection, we determine the local behavior of system (1) when healthy cell population invaded by lobular cancer cell population and in absence of ductal cancer cell population. The lobular cancer invasion equilibrium point is denoted by $\Lambda_1 = (0, T^*_{L1}, 0, I^*_1, E^*_1)$, which is obtained by the following subsystem:

$$\begin{cases} 0 = r_2 T_L\big(C_2 d - a_2 T_L - b_3 I\big) - \delta T_L, \\ 0 = \lambda\mu + I\big(C_4 - a_4 - b_5 T_L\big) - (1-k)\phi_2 IE, \\ 0 = \rho(1-k) - b_7 E. \end{cases} \tag{3}$$

On solving (3), we obtained $\Lambda_1 = (0, T^*_{L1}, 0, I^*_0, E^*_0)$, where $T^*_{L1} = \frac{r_2 C_2 d - b_3 r_2 I^*_1 - \delta}{r_2 a_2}$, $I^*_1 = \frac{\lambda\mu b_7}{(1-k)^2\phi_2\rho - b_7\big(C_4 - a_4 - b_5 T^*_{L1}\big)}$, and $E^*_1 = \frac{(1-k)\rho}{b_7}$.

**Stability of the lobular cancer invasion equilibrium point**

Let us consider the Jacobian matrix of lobular cancer invasion equilibrium point $\Lambda_1 = (0, T^*_{L1}, 0, I^*_1, E^*_1)$, which has the following form

$$J(\Lambda_1) = \begin{pmatrix} m_{11} & 0 & 0 & 0 & 0 \\ m_{21} & m_{22} & 0 & m_{24} & 0 \\ 0 & 0 & m_{33} & 0 & 0 \\ 0 & m_{42} & m_{43} & m_{44} & m_{45} \\ 0 & 0 & 0 & 0 & m_{55} \end{pmatrix},$$

where

$m_{11} = r_1 C_1 - r_1 b_1 T^*_{L1} - \frac{(1-k)^2\phi_1\rho}{b_7}$, $m_{21} = \frac{(1-k)^2\phi_1\rho\varepsilon}{b_7} T^*_{L1}$, $m_{22} = r_2 C_2 d - 2r_2 a_2 T^*_{L1} - r_2 b_3 I^*_1 - \delta$, $m_{24} = -r_2 b_3 T^*_{L1}$, $m_{33} = r_3 C_3 d - r_3 b_4 I^*_1 - \delta$, $m_{42} = -b_5 I^*_1$, $m_{43} = -b_6 I^*_1$, $m_{44} = C_4 - a_4 - b_5 T^*_{L1} - \frac{(1-k)^2\phi_2\rho}{b_7}$, $m_{45} = -(1-k)\phi_2 I^*_1$, $m_{55} = -b_7$.

The characteristic equation of $J(\Lambda_1)$ is given by

$$(m_{11} - \lambda)(m_{33} - \lambda)(m_{55} - \lambda)[\lambda^2 - (m_{22} + m_{44})\lambda + m_{24}m_{42}(R^*_1 - 1)] = 0, \tag{b}$$

where $R^*_1 = \frac{m_{22}m_{44}}{m_{24}m_{42}}$.

**Theorem 2** *Let $\Lambda_1$ be the equilibrium point of system (1) and assume that $R^*_1 > 1$, $\phi_1 > \frac{r_1 C_1 b_7}{\rho(1-k)^2}$ and $\phi_2 > \frac{(C_4 - a_4)b_7}{\rho(1-k)^2}$, then $\Lambda_1$ is locally asymptotically stable if $T^*_{L1} > \frac{(C_4 - a_4)b_7 - (1-k)^2\rho\phi_2}{b_5 b_7}$ and $I^*_1 > \frac{r_2 C_2 d - \delta}{r_2 b_3}$, where $r_3 < \frac{\delta}{C_3 d}$, and $r_2 < \frac{\delta}{C_2 d}$.*

***Proof:*** The characteristic equation of the Jacobian matrix $J(\Lambda_1)$ is $(m_{11} - \lambda)(m_{33} - \lambda)(m_{55} - \lambda)[\lambda^2 - (m_{22} + m_{44})\lambda + m_{24}m_{42}(R^*_1 - 1)] = 0$.

Three eigen values of $J(\Lambda_1)$ are $m_{11} = r_1 C_1 - r_1 b_1 T^*_{L1} - \frac{(1-k)^2\phi_1\rho}{b_7}$, $m_{33} = r_3 c_3 d - r_3 b_4 I^*_1 - \delta$ and $m_{55} = -b_7$.

(i) $m_{55} = -b_7$ is always negative.
(ii) $m_{33} = r_3 C_3 d - r_3 b_4 I^*_1 - \delta < 0$, as $r_3 < \frac{\delta}{C_3 d}$.
(iii) $m_{11} = r_1 C_1 - r_1 b_1 T^*_{L1} - \frac{(1-k)^2\phi_1\rho}{b_7} < 0$, as $\phi_1 > \frac{r_1 C_1 b_7}{\rho(1-k)^2}$.

The remaining two eigen values of the characteristic equation (b) are obtained by $\lambda^2 - (m_{22} + m_{44})\lambda + m_{24}m_{42}(R^*_1 - 1)$. Therefore, stability of $\Lambda_1$ depends on the eigen value of the quadratic equation $\lambda^2 - (m_{22} + m_{44})\lambda + m_{24}m_{42}(R^*_1 - 1)$. On applying Routh–Hurwitz criterion (DeJesus and Kaufman 1987) to the quadratic polynomial, we have the following conditions for locally asymptotically stability of $\Lambda_1$:

$$m_{22} + m_{44} < 0, \text{ and } m_{24}m_{42}(R^*_1 - 1) > 0.$$

We have, $m_{24}m_{42}(R^*_1 - 1) > 0$, and,

$$\begin{aligned} m_{22} + m_{44} &= r_2 C_2 d - 2r_2 a_2 T^*_{L1} - r_2 b_3 I^*_1 - \delta \\ &\quad + C_4 - a_4 - b_5 T^*_{L1} - \frac{(1-k)^2\rho\phi_2}{b_7}, \\ &= \big(r_2 C_2 d - \delta - r_2 b_3 I^*_1\big) \\ &\quad + \left(C_4 - a_4 - \frac{(1-k)^2\rho\phi_2}{b_7} - b_5 T^*_{L1}\right) - 2r_2 a_2 T^*_{L1}. \end{aligned}$$

So, for $m_{22} + m_{44} < 0$, we must have, $r_2 C_2 d - \delta - r_2 b_3 I^*_1 < 0 \Rightarrow I^*_1 > \frac{r_2 C_2 d - \delta}{r_2 b_3}$.

And, $C_4 - a_4 - \frac{(1-k)^2\rho\phi_2}{b_7} - b_5 T^*_{L1} < 0$

$\Rightarrow T^*_{L1} > \frac{(C_4 - a_4)b_7 - (1-k)^2\rho\phi_2}{b_5 b_7}$ for $\phi_2 > \frac{(C_4 - a_4)b_7}{\rho(1-k)^2}$.

Since, $\Lambda_1$ is a positive critical point for $\phi_2 > \frac{(C_4 - \delta)b_7}{\rho(1-k)^2}$, then $\Lambda_1$ is locally asymptotic stable if $T^*_{L1} > \frac{(C_4 - a_4)b_7 - (1-k)^2\rho\phi_2}{b_5 b_7}$, and $I^*_1 > \frac{r_2 C_2 d - \delta}{r_2 b_3}$.

Theorem 2 indicates that with a higher initial value of lobular carcinoma population and low ketogenic diet rate, the lobular cell dominants the cell population and remains in the body. The lobular cancer invasion equilibrium point is asymptotically stable.

### 3.3 Ductal cancer invasion equilibrium point

When ductal carcinoma cells are greater in volume and lobular carcinoma cells are low in volume, lobular cancer cells are not able to compete for resources with ductal cancer cells. Therefore, lobular cell dominants the cancer cell population and invades the total healthy cell population in the body. In this subsection, we determine the local behavior of system (1) when healthy cell population invaded by only ductal cancer cell population in absence of lobular cancer cell population. The lobular cancer invasion equilibrium point is denoted by $\Lambda_2 = (0, 0, T^*_{D2}, I^*_2, E^*_2)$, which is obtained by the following subsystem:

$$\begin{cases} 0 = r_3 T_D\left(C_3 d - a_3 T_D - b_4 I\right) - \delta T_D, \\ 0 = \lambda\mu + I\left(C_4 - a_4 - b_6 T_D\right) - (1-k)\phi_2 IE, , \\ 0 = \rho(1-k) - b_7 E. \end{cases} \tag{4}$$

On solving (4), we obtained $\Lambda_2 = (0, 0, T^*_{D2}, I^*_2, E^*_2)$, where $T^*_{D2} = \frac{r_3 C_3 d - b_4 r_3 I^*_2 - \delta}{r_3 a_3}$, $I^*_2 = \frac{\lambda\mu b_7}{(1-k)^2\phi_2\rho - b_7\left(C_4 - a_4 - b_6 T^*_{D2}\right)}$, and $E^*_2 = \frac{(1-k)\rho}{b_7}$.

**Stability of the ductal cancer invasion equilibrium point**

The Jacobian matrix of the ductal invasion critical point $\Lambda_2 = (0, 0, T^*_{D2}, I^*_2, E^*_2)$ is calculated and denoted by $J(\Lambda_2)$, we obtain, $J(\Lambda_2) = \begin{pmatrix} m_{11} & 0 & 0 & 0 & 0 \\ 0 & m_{22} & 0 & 0 & 0 \\ m_{31} & 0 & m_{33} & m_{34} & 0 \\ 0 & m_{42} & m_{43} & m_{44} & m_{45} \\ 0 & 0 & 0 & 0 & m_{55} \end{pmatrix}$, where

$m_{11} = r_1 C_1 - r_1 b_2 T^*_{D2} - \frac{(1-k)^2\phi_1\rho}{b_7}$ ,

$m_{22} = r_2 C_2 d - r_2 b_3 I^*_2 - \delta$ , $m_{31} = \frac{(1-\varepsilon)(1-k)^2\phi_1\rho T^*_{D2}}{b_7}$ ,

$m_{33} = r_3 C_3 d - 2 r_3 a_3 T^*_{D2} - r_3 b_4 I^*_2 - \delta$ , $m_{34} = -r_3 b_4 T^*_{D2}$ ,

$m_{42} = -b_5 I^*_2$ , $m_{43} = -b_6 I^*_2$ ,

$m_{44} = C_4 - a_4 - b_6 T^*_{D2} - \frac{(1-k)^2\phi_2\rho}{b_7}$ , $m_{45} = -(1-k)\phi_2 I^*_2$

$, m_{55} = -b_7$.

The characteristic equation of the Jacobian $J(\Lambda_2)$ around ductal cancer invasion equilibrium is given by:

$$(m_{11} - \lambda)(m_{22} - \lambda)(m_{55} - \lambda)\left((m_{33} - \lambda)(m_{44} - \lambda) - m_{34}m_{43}\right) = 0, \tag{c}$$

the local stability for $\Lambda_2 = (0, 0, T^*_{D2}, I^*_2, E^*_2)$ is obtained in Theorem 3 as follows:

**Theorem 3** *Let $\Lambda_2 = (0, 0, T^*_{D2}, I^*_2, E^*_2)$ be the equilibrium point of system (1) and assume that $R^*_1 > 1, \phi_1 > \frac{r_1 C_1 b_7}{\rho(1-k)^2}$ and $\phi_2 > \frac{(C_4 - a_4)b_7}{\rho(1-k)^2}$, then $\Lambda_2$ is locally asymptotically stable if $T^*_{D2} > \frac{(C_4 - a_4)b_7 - (1-k)^2\rho\phi_2}{b_5 b_7}$ and $I^*_2 > \frac{r_3 C_3 d - \delta}{r_3 b_4}$, where $r_3 < \frac{\delta}{C_3 d}$, and $r_2 < \frac{\delta}{C_2 d}$.*

***Proof:*** From (c), we obtain three eigen value of the characteristic polynomial as

$\lambda_1 = r_1 C_1 - r_1 b_2 T^*_{D2} - \frac{(1-k)^2\phi_1\rho}{b_7} < 0$ if $\phi_1 > \frac{r_1 C_1 b_7}{(1-k)^2\rho}$.

$\lambda_2 = r_2 C_2 d - r_2 b_3 I^*_2 - \delta < 0$, where $r_2 < \frac{\delta}{c_2 d}$,

and $\lambda_5 = -b_7 < 0$.

Now for the stability of $\Lambda_2$, we need to consider only the quadratic equation:

$$\lambda^2 - (m_{33} + m_{44})\lambda + m_{33}m_{44} - m_{34}m_{43} = 0,$$

which implies,

$\lambda^2 - (m_{33} + m_{44})\lambda + m_{34}m_{43}\left(R^*_2 - 1\right) = 0$, where $R^*_2 = \frac{m_{33}m_{44}}{m_{34}m_{43}}$.

If $R^*_2 > 1$, for both the eigen value of quadratic equation to be negative, we have.

(i) $m_{33} + m_{44} < 0$,
(ii) $m_{33}m_{44} > 0$.

Now on taking $m_{33} + m_{44}$, we have

$$\begin{aligned} m_{33} + m_{44} &= r_3 C_3 d - 2 r_3 a_3 T^*_{D2} - r_3 b_4 I^*_2 - \delta \\ &\quad + C_4 - a_4 - b_6 T^*_{D2} - \frac{(1-k)^2\phi_2\rho}{b_7}, \\ &= \left(r_3 C_3 d - \delta - r_3 b_4 I^*_2\right) \\ &\quad + \left(C_4 - a_4 - \frac{(1-k)^2\rho\phi_2}{b_7} - b_6 T^*_{D2}\right) - 2 r_3 a_3 T^*_{D2}, \end{aligned}$$

so, for $m_{33} + m_{44} < 0$, we must have, $r_3 C_3 d - \delta - r_3 b_4 I^*_2 < 0 \Rightarrow I^*_2 > \frac{r_3 C_3 d - \delta}{r_3 b_4}$ , and , $C_4 - a_4 - \frac{(1-k)^2\rho\phi_2}{b_7} - b_6 T^*_{D2} < 0$,

$\Rightarrow T^*_{D2} > \frac{(C_4 - a_4)b_7 - (1-k)^2\rho\phi_2}{b_6 b_7}$.

Since, $\Lambda_2$ is a positive critical point for $\phi_2 > \frac{(C_4 - \delta)b_7}{\rho(1-k)^2}$, then $\Lambda_2$ is locally asymptotic stable if $T^*_{D2} > \frac{(C_4 - a_4)b_7 - (1-k)^2\rho\phi_2}{b_6 b_7}$, and $I^*_2 > \frac{r_3 C_3 d - \delta}{r_3 b_4}$.

Theorem 3 indicates that with a higher initial value of ductal carcinoma population and low ketogenic diet rate, the ductal cell dominants the cell population and remains in the body. The ductal cancer invasion equilibrium point is asymptotically stable.

### 3.4 Mixed ductal and lobular cancer invasion equilibrium

When ductal carcinoma cells and lobular carcinoma cells are greater in volume, healthy cells are not able to compete for resources with both ductal and lobular cancer cells. Therefore, mixed type of cancer with ductal and lobular characteristics dominants the cancer cell population and invades the total healthy cell population in the body. In this subsection, we determine the local behavior of system (1) when healthy cell population invaded by both ductal and lobular cancer cell population. The lobular cancer invasion equilibrium point is denoted by $\Lambda_3 = (0, T^*_{L3}, T^*_{D3}, I^*_3, E^*_3)$, which is obtained by the following subsystem:

$$\begin{cases} 0 = r_2 T_L\big(C_2 d - a_2 T_L - b_3 I\big) - \delta T_L, \\ 0 = r_3 T_D\big(C_3 d - a_3 T_D - b_4 I\big) - \delta T_D, \\ 0 = \lambda\mu + I\big(C_4 - a_4 - b_5 T_L - b_6 T_D\big) - (1-k)\phi_2 IE, \\ 0 = \rho(1-k) - b_7 E. \end{cases} \tag{5}$$

On solving (5), we obtained $\Lambda_3 = (0, T^*_{L3}, T^*_{D3}, I^*_3, E^*_3)$, where $T^*_{L3} = \frac{r_2 C_2 d - b_3 r_2 I^*_3 - \delta}{r_2 a_2}$, $T^*_{D3} = \frac{r_3 C_3 d - b_4 r_3 I^*_3 - \delta}{r_3 a_3}$, $I^*_2 = \frac{\lambda\mu b_7}{(1-k)^2\phi_2\rho - b_7\left(C_4 - a_4 - b_5 T^*_{L3} - b_6 T^*_{D3}\right)}$, and $E^*_2 = \frac{(1-k)\rho}{b_7}$.

**Stability of mixed ductal and lobular carcinoma**

Let us consider the Jacobian matrix of the dead critical point: $\Lambda_3 = (0, T^*_{L3}, T^*_{D3}, I^*_3, E^*_3)$, now we have

$$J(\Lambda_3) = \begin{pmatrix} m_{11} & 0 & 0 & 0 & 0 \\ m_{21} & m_{22} & 0 & m_{24} & 0 \\ m_{31} & 0 & m_{33} & m_{34} & 0 \\ 0 & m_{42} & m_{43} & m_{44} & m_{45} \\ 0 & 0 & 0 & 0 & m_{55} \end{pmatrix}, \text{where}$$

$m_{11} = r_1 C_1 - r_1 b_1 T^*_{L3} - r_1 b_2 T^*_{D3} - \frac{(1-k)^2\phi_1\rho}{b_7}$,
$m_{21} = \frac{\varepsilon(1-k)^2\phi_1\rho T^*_{L3}}{b_7}$, $m_{22} = r_2 C_2 d - 2r_2 a_2 T^*_{L3} - r_2 b_3 I^*_3 - \delta$,
$m_{24} = -r_2 b_3 T^*_{L3}$, $m_{31} = \frac{(1-\varepsilon)(1-k)^2\phi_1\rho T^*_{D3}}{b_7}$,
$m_{33} = r_3 C_3 d - 2r_3 a_3 T^*_{D3} - r_3 b_4 I^*_3 - \delta$, $m_{34} = -r_3 b_4 T^*_{D3}$,
$m_{42} = -b_5 I^*_3$, $m_{43} = -b_6 I^*_3$,
$m_{44} = C_4 - a_4 - b_5 T^*_{L3} - b_6 T^*_{D3} - \frac{(1-k)^2\phi_2\rho}{b_7}$,
$m_{45} = -(1-k)\phi_2 I^*_3$, $m_{55} = -b_7$.

The characteristic equation of Jacobian $J(\Lambda_3)$ for the mixed lobular ductal cancer invasion equilibrium point is given by:

$$\begin{aligned} &(m_{11} - \lambda)(m_{55} - \lambda)\big((a_{22} - \lambda) \\ &[(a_{33} - \lambda)(a_{44} - \lambda) - a_{34}a_{43}] \\ &-a_{24}a_{42}(a_{33} - \lambda)\big) = 0 \end{aligned} \tag{d}$$

Thus, the local stability for $\Lambda_3 = (0, T^*_{L3}, T^*_{D3}, I^*_3, E^*_3)$ is obtained in Theorem 4 as follows:

**Theorem 4** *Let $\Lambda_3$ be the critical point of system (1) and assume that $\phi_1 > \frac{r_1 C_1 b_7}{(1-k)^2\rho}$, $\phi_2 > \frac{(C_4 - a_4)b_7}{\rho(1-k)^2}$ then $\Lambda_3$ is locally asymptotic stable if and only if $T^*_{L3} > \frac{(C_4 - a_4)b_7 - (1-k)^2\phi_2\rho}{b_5 b_7}$ and $T^*_{D3} > \frac{(C_4 - a_4)b_7 - (1-k)^2\phi_2\rho}{b_6 b_7}$, where $r_2 < \frac{\delta}{C_2 d}$ and $r_3 < \frac{\delta}{C_3 d}$.*

***Proof*** The characteristic equation of Jacobian $J(\Lambda_3)$ is obtained and the eigen values of $J(\Lambda_3)$ are given by:

$\lambda_1 = m_{11} = r_1 C_1 - r_1 b_1 T^*_{L3} - r_1 b_2 T^*_{D3} - \frac{(1-k)^2\phi_1\rho}{b_7} < 0$ if $\phi_1 > \frac{r_1 C_1 b_7}{(1-k)^2\rho}$,
and $\lambda_5 = m_{55} = -b_7 < 0$.

Now, the stability of $\Lambda_3$ depends on the cubic equation, given as:

$$\begin{aligned} &\lambda^3 - (m_{22} + m_{33} + m_{44})\lambda^2 \\ &+ \big(m_{22}m_{33} + m_{22}m_{44} + m_{33}m_{44} - m_{34}m_{43} - m_{24}m_{42}\big)\lambda \\ &- m_{22}m_{33}m_{44} + m_{22}m_{34}m_{43} + m_{24}m_{33}m_{42} = 0, \end{aligned}$$

$$\begin{aligned} \Rightarrow &\lambda^3 - (m_{22} + m_{33} + m_{44})\lambda^2 \\ &+ \big(m_{22}m_{33} + m_{22}m_{44} - m_{24}m_{42} + m_{34}m_{43}(R^*_3 - 1)\big)\lambda \\ &+ m_{24}m_{42}m_{33} - m_{22}m_{34}m_{43}(R^*_4 - 1) = 0, \end{aligned}$$

where, the basic reproduction numbers are $R^*_3 = \frac{m_{33}m_{44}}{m_{34}m_{43}}$ and $R^*_4 = \frac{m_{22}m_{33}m_{44}}{m_{22}m_{34}m_{43}}$.

We apply Routh–Hurwitz criterion (DeJesus and Kaufman 1987) on the cubic equation for the stability of $\Lambda_3$, we get following conditions for the stability of mixed lobular and ductal cancer invasion equilibrium point:

$$m_{22} + m_{33} + m_{44} < 0, \tag{e}$$

$$m_{24}m_{42}m_{33} - m_{22}m_{34}m_{43}(R^*_4 - 1) > 0, \tag{f}$$

$$m_{22}m_{33} + m_{22}m_{44} - m_{24}m_{42} + m_{34}m_{43}(R^*_3 - 1) > 0, \tag{g}$$

and

$$\begin{aligned} &-(m_{22} + m_{33} + m_{44})\big(m_{22}m_{33} + m_{22}m_{44} - m_{24}m_{42} + m_{34}m_{43}(R^*_3 - 1)\big) \\ &> m_{24}m_{42}m_{33} - m_{22}m_{34}m_{43}(R^*_4 - 1). \end{aligned} \tag{h}$$

By Eq. (e), we have,

$$\begin{aligned} &\big(r_2 C_2 d - \delta - r_2 b_3 I^*_3\big) + \big(r_3 C_3 d - \delta - r_3 b_4 I^*_3\big) \\ &- 2r_2 a_2 T^*_{L4} - 2r_3 a_3 T^*_{D3} \\ &+ \left(C_4 - a_4 - b_5 T^*_{L3} - b_6 T^*_{D3} - \frac{(1-k)^2\phi_2\rho}{b_7}\right) < 0, \end{aligned}$$

we have, $r_2 C_2 d - \delta - r_2 b_3 I^*_3 < 0$, and $r_3 C_3 d - \delta - r_3 b_4 I^*_3 < 0$, as $r_2 < \frac{\delta}{C_2 d}$, $r_3 < \frac{\delta}{C_3 d}$, also,

$C_4 - a_4 - b_5 T^*_{L3} - b_6 T^*_{D3} - \frac{(1-k)^2\phi_2\rho}{b_7} < 0$ , if $T^*_{L3} > \frac{(C_4-a_4)b_7-(1-k)^2\phi_2\rho}{b_5 b_7}$ for $\phi_2 > \frac{(C_4-a_4)b_7}{(1-k)^2\rho}$, and $T^*_{D3} > \frac{(C_4-a_4)b_7-(1-k)^2\phi_2\rho}{b_6 b_7}$ for $\phi_2 > \frac{(C_4-a_4)b_7}{(1-k)^2\rho}$.

On the other hand, (f), (g) and (h), satisfies with the condition used in the proof of (e). This completes the proof of Theorem 4.

Theorem 4 indicates that that any decrement in the ketogenic rate enhance the growth of the Mi-DLC population. If the invasion of the lobular and ductal tumor cells into the normal cells is higher, both lobular and ductal cancer cell population dominates the breast tissues, since $\Lambda_3$ depends heavily on higher volume of initial lobular carcinoma and initial ductal carcinoma.

### 3.5 Dead equilibrium point

The dead equilibrium occurs when immune cells and estrogen remains in the human body where the cancer cells and healthy cells are absent. The mortality of human is assured in dead equilibrium condition. The dead equilibrium point $\Lambda_4 = (0, 0, 0, I^*_4, E^*_4)$ is obtained by solving the following equation:

The equilibrium point is obtained by solving (6), denoted by $\Lambda_4 = (0, 0, 0, I^*_4, E^*_4)$, where

$I^*_4 = \frac{\lambda\mu b_7}{(1-k)^2\phi_2\rho - b_7(C_4-a_4)}$, and $E^*_4 = \frac{(1-k)\rho}{b_7}$.

**Stability of dead equilibrium point**

The Jacobian matrix of the dead critical point $\Lambda_4 = (0, 0, 0, I^*_4, E^*_4)$ is given by:

$$J(\Lambda_4) = \begin{pmatrix} m_{11} & 0 & 0 & 0 & 0 \\ 0 & m_{22} & 0 & 0 & 0 \\ 0 & 0 & m_{33} & 0 & 0 \\ 0 & m_{42} & m_{43} & m_{44} & m_{45} \\ 0 & 0 & 0 & 0 & m_{55} \end{pmatrix},$$

where

$m_{11} = r_1 C_1 - \frac{(1-k)^2\phi_1\rho}{b_7}$, $m_{22} = r_2 C_2 d - r_2 b_3 I^*_3 - \delta$, $m_{33} = r_3 C_3 d - r_3 b_4 I^*_3 - \delta$, $m_{42} = -b_5 I^*_3$, $m_{43} = -b_6 I^*_3$, $m_{44} = C_4 - a_4 - \frac{(1-k)^2\phi_2\rho}{b_7}$, $m_{45} = -(1-k)\phi_2 I^*_3$, $m_{55} = -b_7$.

The characteristic equation of Jacobian $J(\Lambda_4)$ is

$$(m_{11} - \lambda)(m_{22} - \lambda)(m_{33} - \lambda)(m_{44} - \lambda)(m_{55} - \lambda) = 0 \quad \text{(i)}$$

**Theorem 5** *Assume that* $\phi_1 > \frac{r_1 C_1 b_7}{(1-k)^2\rho}$ *and* $\phi_2 > \frac{(C_4-\delta)b_7}{(1-k)^2\rho}$ *holds. The dead critical point* $\Lambda_3$ *of system* (1) *is stable local asymptotic if* $r_2 < \frac{\delta}{C_2 d}$, *and* $r_3 < \frac{\delta}{C_3 d}$.

***Proof*** From (i), we obtain the following five eigen values of Jacobian $J(\Lambda_4)$:

(i) $\lambda_1 = r_1 C_1 - \frac{(1-k)^2\phi_1\rho}{b_7} < 0$ if $\phi_1 > \frac{r_1 C_1 b_7}{(1-k)^2\rho}$.

(ii) $\lambda_2 = r_2 C_2 d - \delta - r_2 b_3 I < 0$, as $r_2 < \frac{\delta}{C_2 d}$.

(iii) $\lambda_3 = r_3 C_3 d - \delta - r_3 b_4 I < 0$, as $r_3 < \frac{\delta}{C_3 d}$.

$$\begin{cases} 0 = \lambda\mu + I\big(C_4 - a_4\big) - (1-k)\phi_2 IE, \\ 0 = \rho(1-k) - b_7 E. \end{cases} \quad (6)$$

(iv) $\lambda_4 = -\frac{(1-k)^2\phi_2\rho - b_7(C_4-a_4)}{b_7} < 0$ since $\phi_2 > \frac{(C_4-\delta)b_7}{(1-k)^2\rho}$.

(v) $\lambda_5 = -b_7 < 0$.

Theorem 5 indicates that if the immune suppression rate due to high estrogen is high in body, and tumor growth rate is higher with more DNA damage, the both mixed ductal and lobular cancer cells invades the healthy population and the death of human is assured. The dead equilibrium $\Lambda_4$ is asymptotically stable.

### 3.6 Co-existing equilibrium point

Coexisting equilibrium points arise when there steady-state solutions for the system of differential equations. In the mathematical model for Mi-DLC, coexisting equilibrium points arises when the tumor cells move to a dormant state and stops invading the healthy cells population. In that state the lobular cancer ductal cancer stays with healthy cells population with very minimum volume. A dynamical system in system (1) containing mathematical model of mixed invasive ductal and lobular carcinoma (Mi-DLC) with Healthy cells, lobular cancer cell, ductal cancer cell, estrogen hormones, and immune responses possibly have coexisting equilibrium points. The equilibrium points of co-existing state are obtained by.

**Stability of coexisting equilibrium point**

Let us consider the Jacobian matrix of the co-existing critical point: $\Lambda_5 = (H^*_5, T^*_{L5}, T^*_{D5}, I^*_5, E^*_5)$.

Which has the form

$$J(\Lambda_5) = \begin{pmatrix} m_{11} & m_{12} & m_{13} & 0 & m_{15} \\ m_{21} & m_{22} & 0 & m_{24} & m_{25} \\ m_{31} & 0 & m_{33} & m_{34} & m_{35} \\ 0 & m_{42} & m_{43} & m_{44} & m_{45} \\ 0 & 0 & 0 & 0 & m_{55} \end{pmatrix},$$ where,

$m_{11} = r_1 c_1 - 2r_1 a_1 H - r_1 b_1 T_L - r_1 b_2 T_D - \frac{(1-k)^2\phi_1\rho}{b_7}$, $m_{12} = -r_1 b_1 H$, $m_{13} = -r_1 b_2 H$, $m_{15} = -(1-k)\phi_1 H$, $m_{21} = \frac{\varepsilon(1-k)^2\phi_1\rho T_L}{b_7}$, $m_{22} = r_2 c_2 d - 2r_2 a_2 T_L - r_2 b_3 I - \delta + \frac{\varepsilon(1-k)^2\phi_1\rho H}{b_7}$, $m_{24} = -r_2 b_3 T$, $m_{25} = \varepsilon(1-k)\phi_1 H T_L$, $m_{31} = \frac{(1-\varepsilon)(1-k)^2\phi_1\rho T_D}{b_7}$, $m_{33} = r_3 c_3 d - 2r_3 a_3 T_D - r_3 b_4 I - \delta + \frac{(1-\varepsilon)(1-k)^2\phi_1\rho H}{b_7}$, $m_{34} = -r_3 b_4 T_D$, $m_{35} = (1-\varepsilon)(1-k)\phi_1 H T_D m_{42} = -b_5 I$,

$m_{43} = -b_6 I$ , $m_{44} = c_4 - a_4 - b_5 T_L - b_6 T_D - \frac{(1-k)^2 \phi_2 \rho}{b_7}$ ,
$m_{45} = -(1-k)\phi_2 I, m_{55} = -b_7.$

If we have one eigen value as,

$$\lambda_5 = -b_7 < 0$$

So, characteristic equation of $J(\Lambda_5)$ is a bi-quadratic equation of the form $ch\left(J\left(\Lambda_5\right)\right) = \lambda^4 + a_3\lambda^3 + a_2\lambda^2 + a_1\lambda + a_0$, where,

$a_3 = (-m_{11} - m_{22} - m_{33} - m_{44})$,

$a_2 = (m_{11}m_{44} + m_{22}m_{33} + m_{12}m_{21}(R_5^* - 1) + m_{13}m_{31}(R_6^* - 1) + m_{34}m_{43}(R_7^* - 1) + m_{24}m_{42}(R_8^* - 1))$,

$$\begin{aligned} a_1 = &(m_{33}m_{24}m_{42} + m_{11}m_{24}m_{42} + m_{13}m_{31}m_{22} \\ &+ m_{44}m_{13}m_{31} - m_{11}m_{34}m_{43}(R_7^* - 1) - m_{12}m_{21}m_{33}(R_5^* - 1) \\ &- m_{12}m_{21}m_{44}(R_5^* - 1) - m_{22}m_{34}m_{43}(R_7^* - 1)), \end{aligned}$$

$$\begin{aligned} a_0 = &(m_{11}m_{22}m_{33}m_{44} - m_{11}m_{22}m_{34}m_{43} - m_{11}m_{24}m_{33}m_{42} \\ &- m_{12}m_{21}m_{33}m_{44} + m_{12}m_{21}m_{34}m_{43} - m_{12}m_{24}m_{31}m_{43} \\ &- m_{13}m_{21}m_{34}m_{42} - m_{13}m_{22}m_{31}m_{44} + m_{13}m_{24}m_{31}m_{42}), \end{aligned}$$

and, $R_5^* = \frac{m_{11}m_{22}}{m_{12}m_{21}}$, $R_6^* = \frac{m_{11}m_{33}}{m_{13}m_{31}}$, $R_7^* = \frac{m_{33}m_{44}}{m_{34}m_{43}}$, and, $R_8^* = \frac{m_{22}m_{44}}{m_{24}m_{42}}$.

By Routh–Hurwitz criterion (Oke et al. 2018), the equilibrium state $\Lambda_5$ is stable if following conditions are met:

(i) $a_3 > 0, a_0 > 0$
(ii) $a_3 a_2 > a_1$,
(iii) $(a_3 a_2 - a_1)a_1 - a_3^2 a_0 > 0$.

By applying the value of default parameters taken in Table 1, we observe that condition (i), (ii) and (iii) are satisfied if we take $d = 0.11$ day$^{-1}$ and increasing the dosage of anticancer drugs in body. So, on considering the default parameters with proper ketogenic diet and all other control parameters in humans the Mi-DLC moves to dormant state and do not proliferate further to invade more healthy cells in breast tissue.

## 4 Numerical simulation

In the numerical simulation section, we perform the simulation of system (1), and obtain the numerical results to validate and demonstrate the analytical results of system (1). We show the dynamics of system (1) to show the stability of equilibrium points. We used all the default values of parameters defined in Table 1 to perform the simulation.

The healthy cell population competes with both lobular and ductal cancer cell for resources and immune cells in the form of natural killer cells and CD8+ T-cells attacks the lobular and ductal cells. Initially, individuals do not strictly adopt ketogenic diet, but over time, a portion of fat, carbs, and protein corresponding to the ideal ketogenic diet is gradually introduced into their daily meals based on their body weight. Therefore, an initial ketogenic diet rate of 0.03 per day is adopted in the proposed model. However, it's important to note that increasing the ketogenic diet rate can lead to a condition known as ketoacidosis, which is a combination of ketosis and acidosis. Ketosis involves the production of ketone bodies, while acidosis refers to increased acidity in the blood, resulting in symptoms such as frequent urination, decreased appetite, and even loss of consciousness. Also, participants following a very-low-carbohydrate ketogenic diet had a significantly greater increase in low-density lipoprotein cholesterol (LDL-C) levels when compared to participants following a low-fat diet at 95% level of significance: with ketogenic diet intake rate from 0.03 to $-0.3$, having p value of 0.002 (Batch et al. 2020). The higher increment in ketogenic diet intake rate may subsequently lead to the development of accelerated atherosclerosis and increases the risks associated with cardiovascular disease (Batch et al. 2020). Hence, a high ketogenic diet rate of 0.33 per day is considered as acceptable and appropriate in treatment process, and this interaction can potentially be supported by anti-cancer drugs such as tamoxifen.

The lobular cell population and ductal cell population grows exponentially to invade the healthy cell population. In the initial stage where both the lobular cancer cells and ductal cancer cells are low in volume, the cancer-free equilibrium is stable with high ketogenic diet rate. Figure 2 represents the stability of cancer-free equilibrium state by numerical simulation of system (1) with initial conditions as $H(0) = 0.55 \times 10^6\ cells, T_L(0) = 0.3 \times 10^6 cells$, $T_D(0) = 0.2 \times 10^6 cells$ , $I(0) = 0.7 \times 10^6 cells$ , $E(0) = 0.1 \times 10^1$ µg/ml and the ketogenic diet rate is taken as $d = 0.33$ day$^{-1}$.

Figure 3 represent the stability of mixed lobular and ductal cancer invasion equilibrium, when we take low ketogenic diet rate $d = 0.03$ day$^{-1}$ and, initial conditions are $H(0) = 0.55 \times 10^6 cells, T_L(0) = 0.7 \times 10^6 cells$, $T_D(0) = 0.6 \times 10^6 cells$ , $I(0) = 0.7 \times 10^6 cells$ , and $E(0) = 0.1 \times 10^1$ µg/ml.

We can observe from Figs. 2 and 3 that the high ketogenic diet rate results in stability of cancer-free state. The logistic bifurcation map of lobular cell population and ductal cell population is simulated with low ketogenic diet rate and high ketogenic diet rate.

Figure 4 shows that after a specific time the ductal cell population becomes denser and higher that immune system needs additional support from any control parameters. Figure 5 shows the population size decreases with higher ketogenic diet rate $d = 0.33$ day$^{-1}$ and with other control parameters including anticancer drug tamoxifen.

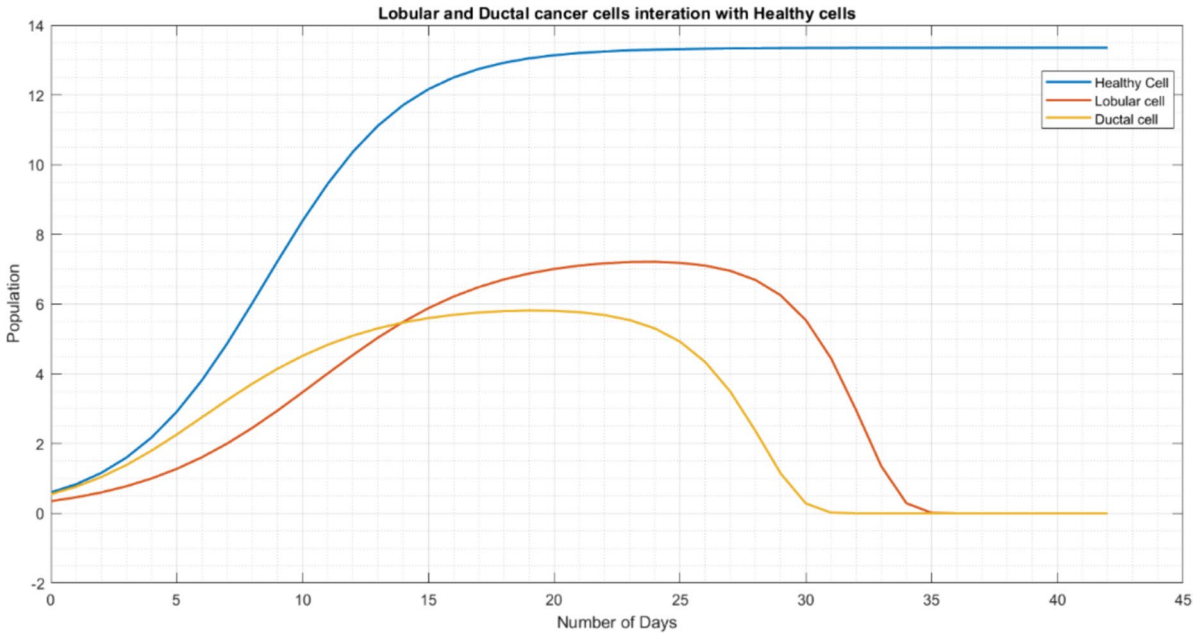


**Fig. 2** The time series diagram showing the stability of cancer-free equilibrium state

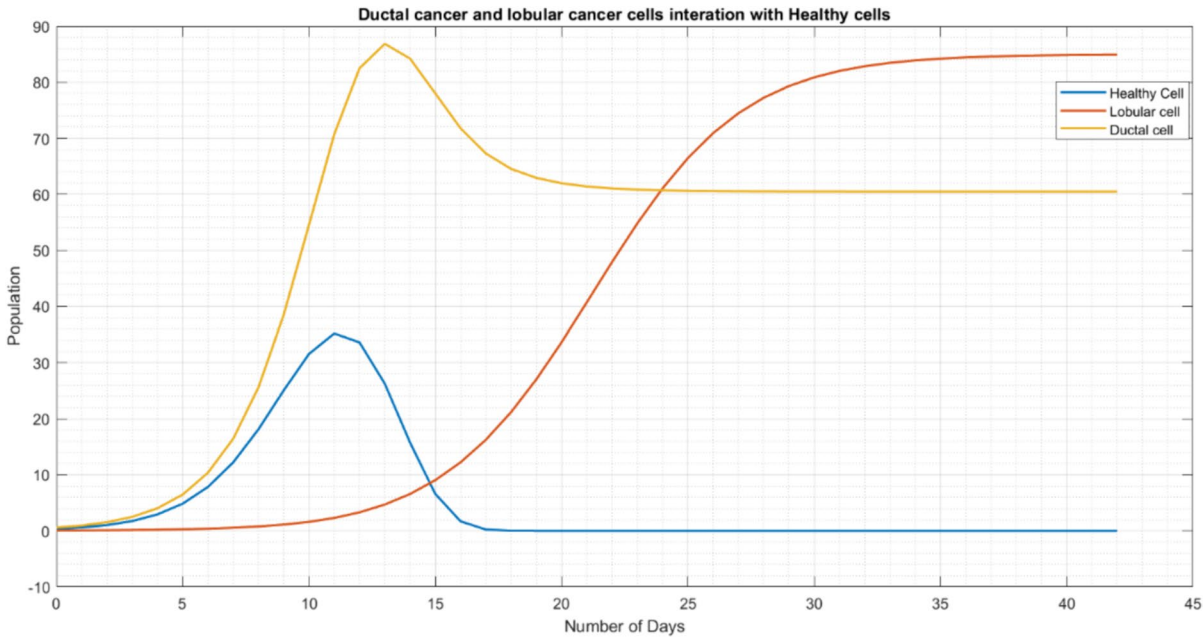


**Fig. 3** The time series diagram showing the stability of mixed ductal and lobular cancer invasion equilibrium

Figure 5 indicates that with same growth rate of ductal cancer cells the increment of 10% in ketogenic diet rate results in inhibition of cancer cells by 60%.

The lobular cancer cell population with lower ketogenic diet rate $d = 0.03\ \text{day}^{-1}$ is shown in Fig. 6. The lobular population is dense and increased highly without any control parameter.

The higher rate of ketogenic diet results in suppression of lobular cancer cell population. The high ketogenic diet rate $d = 0.33\ \text{day}^{-1}$ with tamoxifen is applied to lobular

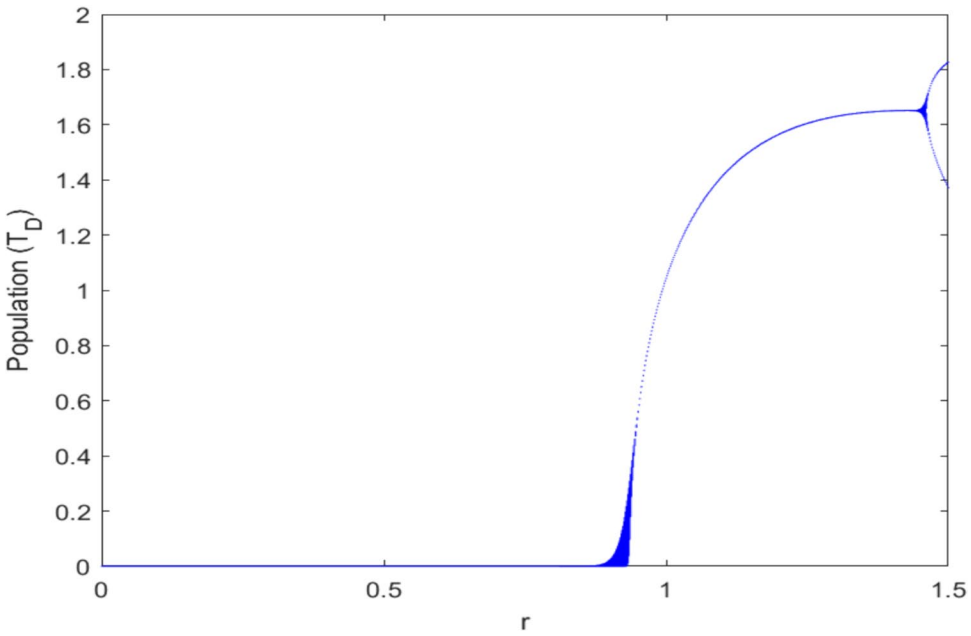


**Fig. 4** The logistic bifurcation diagram of invasive ductal cancer cell population

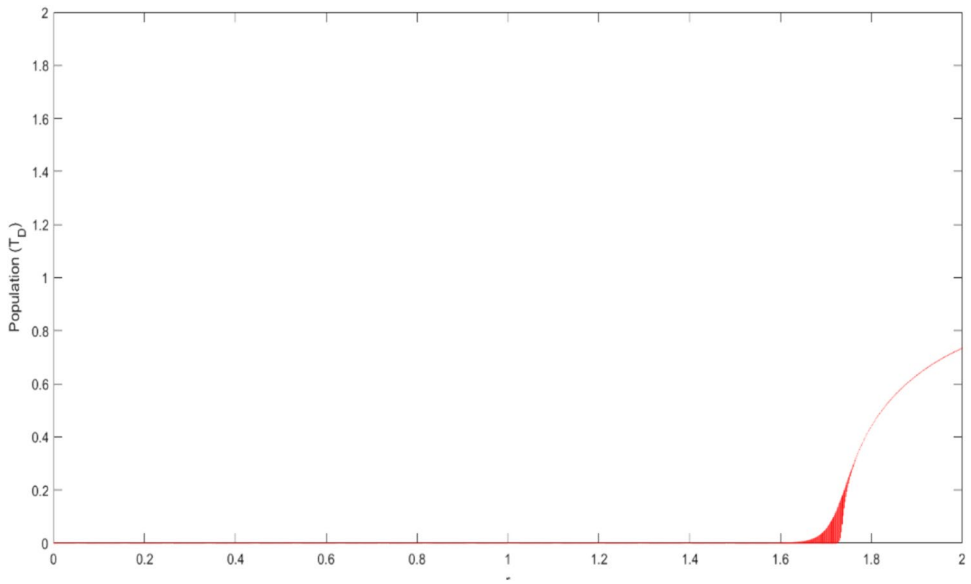


**Fig. 5** The logistic bifurcation diagram of invasive ductal cancer cell population with higher ketogenic diet rate

population logistic growth and the inhibition of lobular cell is shown in Fig. 7.

It is visible in Fig. 7 that 10% increment of ketogenic diet rate results in 70% decrement in lobular cancer cell population. Numerical simulation established that ketogenic diet with other control parameters including anticancer drug tamoxifen significantly reduces both lobular and ductal cancer cell population.

For better understanding of the controls strategy, comparison of the results from both the positive control is performed with the help of numerical simulation of the model.

For a low ketogenic diet rate of 0.03 $day^{-1}$, the numerical simulation of the system (1) demonstrates the ductal cancer cell population in the presence and absence of anticancer drugs in Fig. 8.

In Fig. 8, we observe a sudden spike in the time series graph of the ductal cancer cell population in the absence of anticancer drugs, which indicates that the low ketogenic diet rate leads to very aggressive tumor proliferation in the absence of anticancer drugs as compared to the presence of anticancer drugs as treatment.

For the ductal cancer cell population, Fig. 9 illustrates the high rate of ketogenic diet in combination with anticancer drugs effectively suppresses the proliferation of ductal cancer cells compared to treatment without anticancer drugs (Fig. 9 attached herewith).

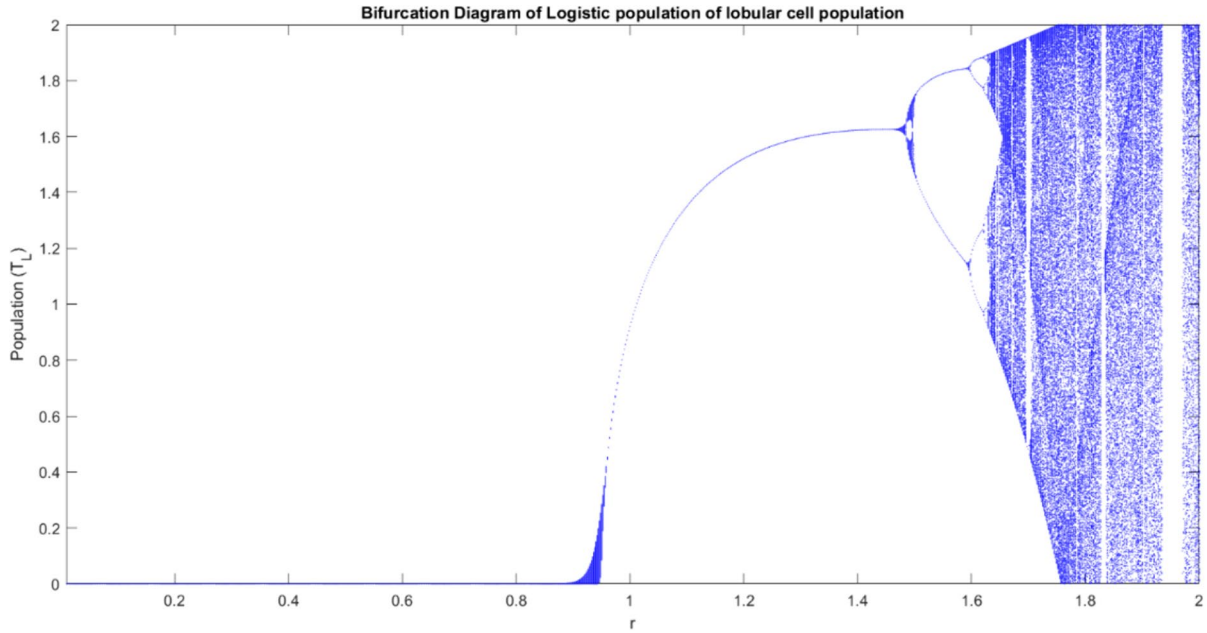


**Fig. 6** The logistic bifurcation diagram of invasive lobular cancer cell population

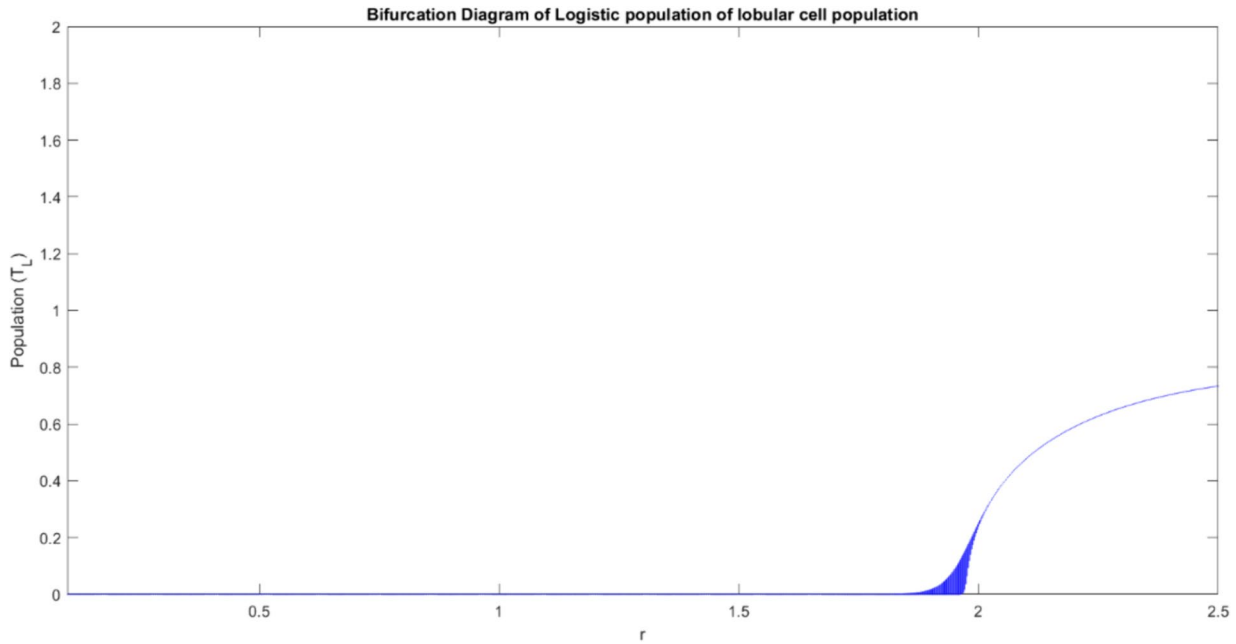


**Fig. 7** The logistic bifurcation diagram of invasive lobular cancer cell population with higher ketogenic diet rate

Therefore, Figs. 8 and 9 clearly show the significant reduction in ductal cancer proliferation achieved by the combined treatment of high ketogenic diet and anticancer drugs in human.

Similarly, for the lobular cancer cell population, Fig. 10 demonstrates the aggressive growth of lobular cancer cells in the absence of anticancer drugs with a low ketogenic diet rate of 0.03 $day^{-1}$, whereas the inhibition of proliferation is observed in the presence of anticancer drugs. Also, Fig. 11 shows the high ketogenic diet rate leads to a decrease in the proliferation rate of lobular cancer with anticancer drugs.

Therefore, Figs. 10 and 11 clearly show the inhibition of the lobular cancer cell population in the presence of anticancer drugs in combination with high ketogenic diet rate in human.

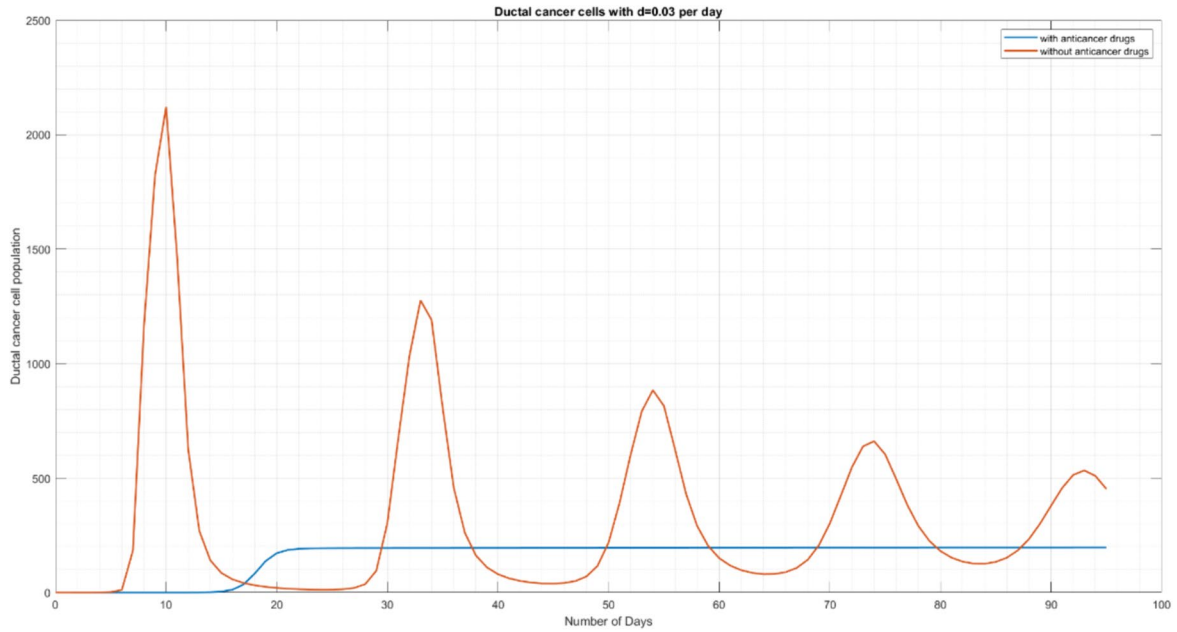


**Fig. 8** The time series graph of ductal cancer cell population with low ketogenic diet rate

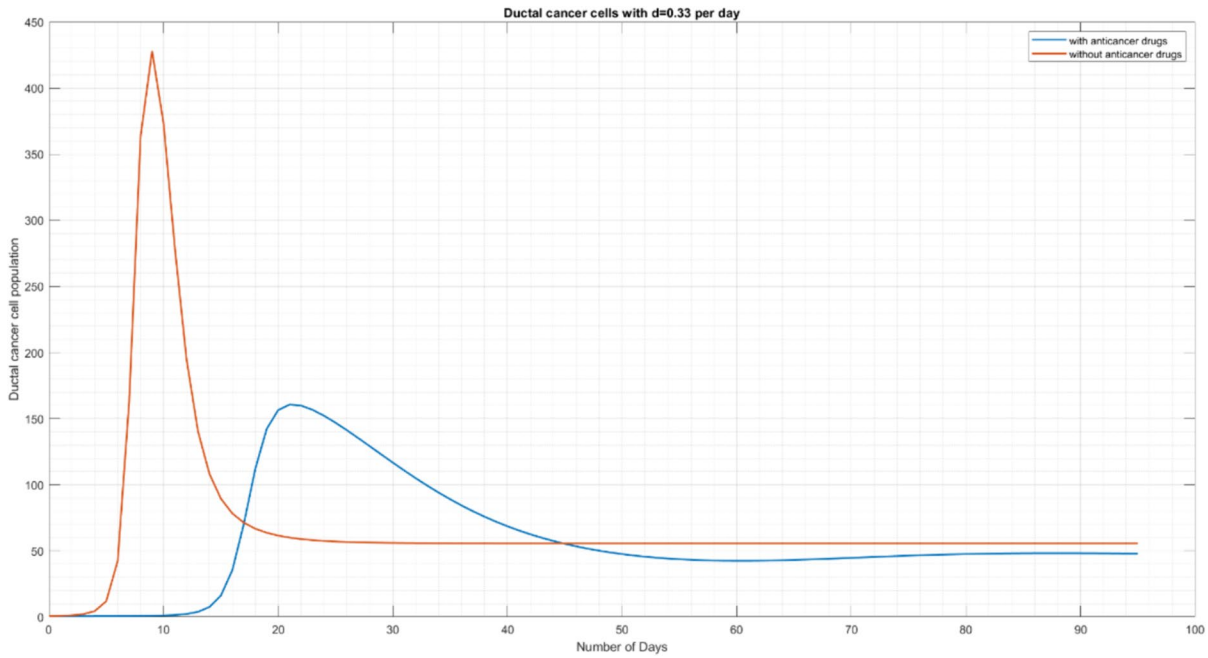


**Fig. 9** The time series graph of ductal cancer cell population with high ketogenic diet rate

## 5 Discussion

Breast cancer is the leading cause of mortality in women around the world. The mixed invasive ductal and lobular cancer (Mi-DLC) is the type of breast cancer which shows both ductal and lobular cancer morphology. The Metastatic behavior of the Mi-DLC has been studied well theoretically and clinically. The theoretical study of the invasion of cancer in the healthy organs through metastasis is most crucial to apply any control strategy. To understand the behavior of Mi-DLC, and to find control parameters for inhibition of the

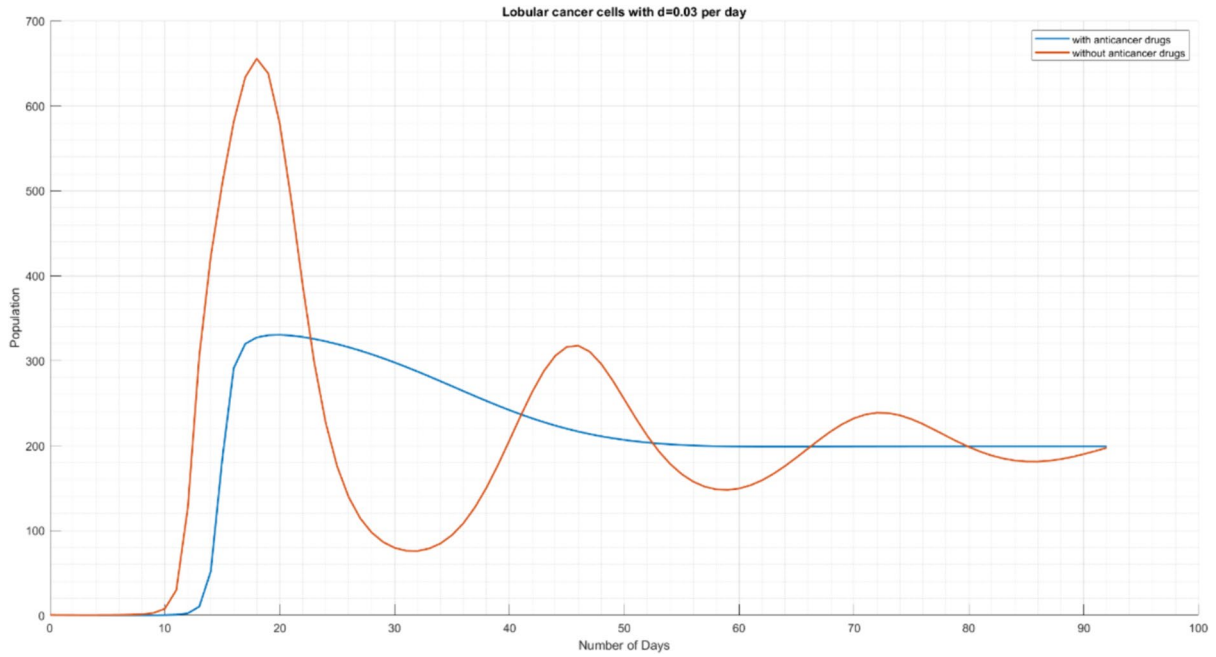


**Fig. 10** The time series graph of lobular cancer cell population with low ketogenic diet rate

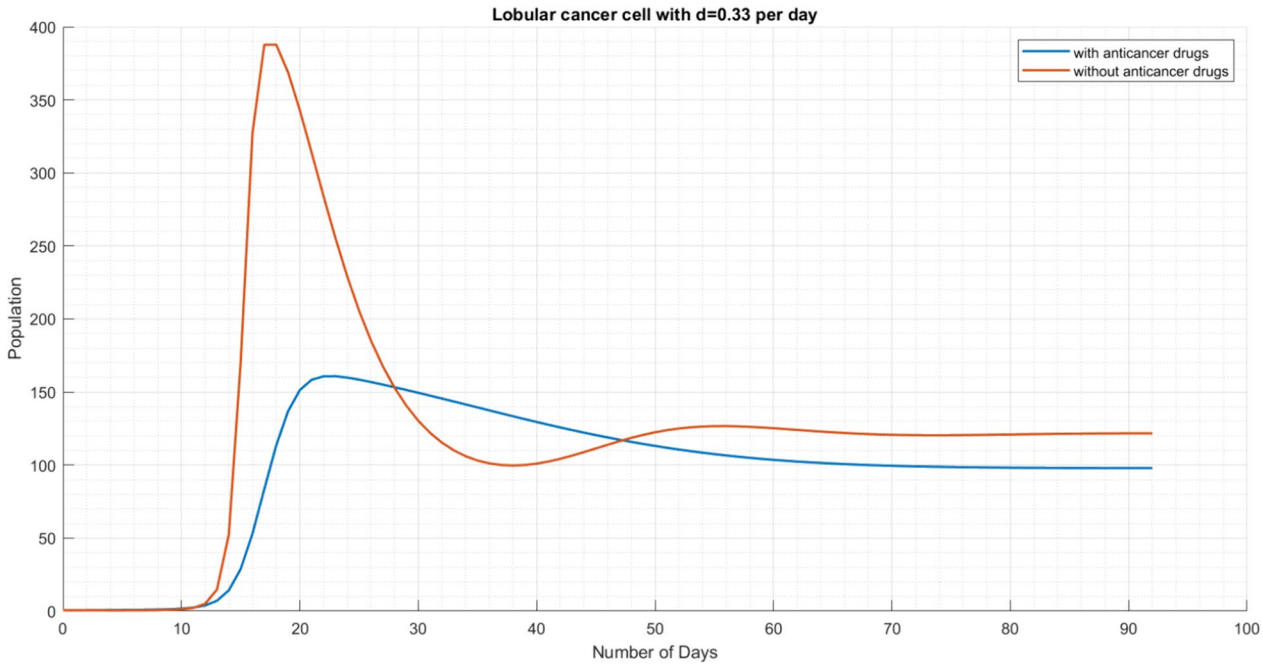


**Fig. 11** The time series graph of lobular cancer cell population with high ketogenic diet rate

tumor cell population, we proposed a mathematical model of tumor immune interaction with healthy cell population in presence of estrogen hormone. The interaction between healthy cell and both ductal and lobular cancer cell has been incorporated in the model. the immune response is studied through the interaction of immune cells population with healthy cell, lobular cancer cell and ductal cancer cell. The usage of anticancer drug tamoxifen and immune booster have been studied through the model. The ketogenic diet is introduced in the model to study the effect of ketogenic diet and anticancer drug therapy in the inhibition of tumor proliferation. In Sect. 3, we have studied the equilibrium

states of the proposed model. The model contained a stable cancer-free equilibrium when the ketogenic diet rate is high in the body with anticancer drugs are provided to the cases. We investigated that if initial value of lobular carcinoma population is high and ketogenic diet rate is low, then lobular cell dominants the cell population in a person even with the dosage of anticancer drugs. So, the lobular cancer invasion equilibrium point is asymptotically stable if initial population of lobular cell is high and ketogenic diet rate is low in human body. Also, the ductal cancer invasion equilibrium point is asymptotically stable if initial population of ductal cell is high and ketogenic diet rate is low in human body. We showed that, if the ketogenic diet rate slightly decreased in a human body, the ductal and lobular cell both invades the healthy cell population. The stability of mixed ductal and lobular invasion equilibrium depends heavily on the initial value of ductal and lobular cell population in the body. We have observed that the immune system response is not sufficient to control the growth of Mi-DLC. The use of anticancer drugs with low ketogenic diet rate does not significantly suppress the proliferation of tumor cells. The introduction of ketogenic diet in humans with proper anticancer drug therapy leads to cancer-free condition in human body. In numerical simulation section we discovered that when the initial cell population size of both lobular and ductal cancer is considered with high ketogenic diet rate and proper anticancer drug therapy, the cancer-free equilibrium state is stable. Figure 2 shows the stability of cancer-free equilibrium state with $d = 0.33\ \text{day}^{-1}$. Figure 3 represent the stability of mixed ductal and lobular invasion equilibrium state. The Fig. 3 shows that when ketogenic diet rate is low i.e., the person with Mi-DLC is not following the ketogenic diet, the lobular and ductal cancer proliferate and invade the healthy cell population. We discovered that with all the control parameters and anticancer drug therapy, the use of ketogenic diet is most effective in inhibition of cancer proliferation. Figures 4 and 5 represent bifurcation diagram of the logistic growth of ductal carcinoma cells population. We discovered that the 10% increment in ketogenic diet rate reduces the proliferation of ductal cancer cell by 60%. Figures 6 and 7 represent the bifurcation diagram of the logistic growth of lobular carcinoma cell population. Figures 6 and 7 indicates that the immune system response and anticancer drug therapy is not sufficient to control the proliferation of tumor cell but the 10% increment of ketogenic diet rate reduces the lobular cancer proliferation by 70%. We compare the use of a ketogenic diet with anticancer drugs as treatment strategies of Mi-DLC. Figures 8 and 9 clearly show the significant reduction in ductal cancer proliferation achieved by the combined treatment of high ketogenic diet and anticancer drugs in human. Also, Figs. 10 and 11 clearly show the inhibition of the lobular cancer cell population in the presence of anticancer drugs in combination with high ketogenic diet rate in human. Therefore, the simulation of the model clearly demonstrates that the use of anticancer drugs alone is insufficient to effectively inhibit mixed invasive ductal and lobular cancer proliferation. However, when combined with a high ketogenic diet, the proper use of anticancer drugs proves highly effective in controlling the high growth rate of the tumor.

We acknowledge few limitations of the mathematical model to be applied on the real-world scenario. Although mathematical models cannot fully substitute doctors, they can effectively aid in the prevention techniques (Li et al. 2023). The present work relies on assumptions of a model. The model assumes that the lobular and ductal cancer both proliferate simultaneously and interact with healthy cells together. The model is built on assumptions about the interactions between ductal and lobular carcinoma cells. These assumptions may not accurately represent the intricacies of cellular crosstalk, microenvironmental influences, or the dynamic changes in cell behavior over time. The assessment of controversial conditions by doctors involves subjectivity, and more complex characteristics can further impact the prevention techniques. Model's predictions for mixed invasive ductal and lobular carcinoma are challenging due to the limited availability of comprehensive clinical data on this specific subtype. The lack of extensive datasets for model validation introduces uncertainties in its predictive capabilities. However, a multidisciplinary approach that combines mathematical modeling with clinical observations, molecular biology insights, and ongoing research efforts are needed to better understand and predict the behavior of mixed invasive ductal and lobular carcinoma. However, having the challenges in capturing the full complexity of mixed invasive ductal and lobular carcinoma, the mathematical model provides valuable insights into the overall dynamics of the tumor. It can reveal general trends and behaviors that contribute to a better understanding of the disease. Finally, the metastatic behavior of Mi-DLC is observed through mathematical model and the positive effect of ketogenic diet with various control parameters. The proposed model can generate hypotheses and predictions that guide further experimental and clinical research. Also, the proposed model allows for the quantitative assessment of outcomes from the ketogenic diet in treatment of Mi-DLC, enabling researchers and clinicians to predict and evaluate the effectiveness of ketogenic diet with other control parameters and anticancer drug therapy for mixed invasive ductal and lobular carcinoma.

## 6 Conclusion

Breast cancer has been the most common type of cancer in humans worldwide. Mixed invasive ductal and lobular carcinoma (Mi-DLC) is a type of breast cancer with both ductal and lobular morphology. We developed the nonlinear deterministic mathematical model to analyze and control the metastatic behavior of Mi-DLC. We incorporated estrogen in the competition among the population of healthy cells, lobular cells, ductal cells, and immune cells. The ketogenic diet has been linked with the metabolism of cancer cells. So, the use of a ketogenic diet in the inhibition of cancer growth has been observed for Mi-DLC. We obtained a stable cancer-free equilibrium state by increasing the ketogenic diet rate along with the use of anticancer drugs in humans. We observed that the immune response of humans is incapable of fighting the disease when the initial volume of Mi-DLC is high and the ketogenic diet rate is low in the body. The model has four cancer invasion equilibriums: lobular cancer invasion, ductal cancer invasion, mixed ductal and lobular invasion, and dead equilibrium state. We found cancer invasion equilibrium states to be stable when we consider a low rate of ketogenic diet with a high initial volume of cancer cells in the body. We calculated that co-existing equilibrium is stable with the proper use of anticancer drugs and a high ketogenic diet rate in humans. The numerical simulation supported the mathematical analysis of the model and established that the 10% increase in ketogenic diet rate leads to the inhibition of both lobular and ductal tumor cells by 60% and 70%, respectively. The model explored that the ketogenic diet, with all the other therapies together, is a promising adjuvant to inhibit the growth of tumors. In the future, we could find the effect of the ketogenic diet rate with immunotherapy and chemotherapy on the growth of Mi-DLC, which can be used as a milestone for preventing breast cancer.

**Acknowledgements** The authors are extremely thankful, to the Department of Mathematics, National Institute of Technology Raipur (C. G.), India, for providing facilities, space, and an opportunity for the work.

**Data availability** All parameters used in the model which support the findings of this study are included within this paper.

## References

Arpino G, Bardou VJ, Clark GM, Elledge RM (2004) Infiltrating lobular carcinoma of the breast: tumor characteristics and clinical outcome. Breast Cancer Res BCR 6(3):R149–R156. https://doi.org/10.1186/bcr767

Batch JT, Lamsal SP, Adkins M, Sultan S, Ramirez MN (2020) Advantages and disadvantages of the ketogenic diet: a review article. Cureus 12(8):e9639. https://doi.org/10.7759/cureus.9639

De Pillis LG, Radunskaya A (2001) A mathematical tumor model with immune resistance and drug therapy: an optimal control approach. Comput Math Methods Med 3(2):79–100

De Pillis LG, Radunskaya A (2003) A mathematical model of immune response to tumor invasion. Comput Fluid Solid Mech. https://doi.org/10.1016/B978-008044046-0.50404-8

DeJesus EX, Kaufman C (1987) Routh–Hurwitz criterion in the examination of eigenvalues of a system of nonlinear ordinary differential equations. Phys Rev A Gen Phys 35(12):5288–5290. https://doi.org/10.1103/physreva.35.5288

DeSantis C, Siegel R, Bandi P, Jemal A (2011) Breast cancer statistics, 2011. CA Cancer J Clin 61(6):409–418. https://doi.org/10.3322/caac.20134

Furukawa K, Shigematus K, Iwase Y, Mikami W, Hoshi H, Nishiyama T, Ohtuka A, Abe H (2018) Clinical effects of one year of chemotherapy with a modified medium-chain triglyceride ketogenic diet on the recurrence of stage IV colon cancer. J Clin Oncol 36(15):e15709–e15709. https://doi.org/10.1200/JCO.2018.36.15_suppl.e15709

Harper JC, Aittomäki K, Borry P, Cornel MC, de Wert G, Dondorp W, Geraedts J, Gianaroli L, Ketterson K, Liebaers I, Lundin K, Mertes H, Morris M, Pennings G, Sermon K, Spits C, Soini S, van Montfoort APA, Veiga A, Vermeesch JR, Viville S, Macek M Jr, on behalf of the European Society of Human Reproduction and Embryology and European Society of Human Genetics (2018) Recent developments in genetics and medically assisted reproduction: from research to clinical applications. Eur J Hum Genet EJHG 26(1):12–33. https://doi.org/10.1038/s41431-017-0016-z

Kim JM (2017) Ketogenic diet: old treatment, new beginning. Clin Neurophysiol Pract 2:161–162. https://doi.org/10.1016/j.cnp.2017.07.001

Klement RJ (2018) Fasting fats, and physics: combining ketogenic and radiation therapy against cancer. Complement Med Res 25(2):102–113. https://doi.org/10.1159/000484045

Klement RJ, Sweeney RA (2016) Impact of a ketogenic diet intervention during radiotherapy on body composition: I. Initial clinical experience with six prospectively studied patients. BMC Res Notes 9:143. https://doi.org/10.1186/s13104-016-1959-9

Knútsdóttir H, Pálsson E, Edelstein-Keshet L (2014) Mathematical model of macrophage-facilitated breast cancer cells invasion. J Theor Biol 357:184–199. https://doi.org/10.1016/j.jtbi.2014.04.031

Lee WL, Cheng MH, Chao HT, Wang PH (2008) The role of selective estrogen receptor modulators on breast cancer: from tamoxifen to raloxifene. Taiwan J Obstet Gynecol 47(1):24–31. https://doi.org/10.1016/S1028-4559(08)60051-0

Li CI, Uribe DJ, Daling JR (2005) Clinical characteristics of different histologic types of breast cancer. Br J Cancer 93(9):1046–1052. https://doi.org/10.1038/sj.bjc.6602787

Li L, Deng H, Ye X, Li Y, Wang J (2023) Comparison of the diagnostic efficacy of mathematical models in distinguishing ultrasound imaging of breast nodules. Sci Rep 13:16047. https://doi.org/10.1038/s41598-023-42937-x

Mayo Clinic (2023) Breast cancer types: what your type means. https://www.mayoclinic.org/diseases-conditions/breast-cancer/in-depth/breast-cancer/art-20045654. Accessed 29 Sept 2023

Metzger-Filho AO, Ferreira AR, Jeselsohn R, Barry WT, Dillon DA, Brock JE, Vaz-Luis I, Hughes ME, Winer EP, Lin NU (2019) Mixed invasive ductal and lobular carcinoma of the breast: prognosis and the importance of histologic grade. Oncologist 24(7):e441–e449. https://doi.org/10.1634/theoncologist.2018-0363

Mirzaei NM, Su S, Sofia D, Hegarty M, Abdel-Rahman MH, Asadpoure A, Cebulla CM, Chang YH, Hao W, Jackson PR, Lee AV, Stover DG, Tatarova Z, Zervantonakis IK, Shahriyari L (2021) A mathematical model of breast tumor progression based on

immune infiltration. J Personal Med 11:10. https://doi.org/10.3390/jpm11101031

Mufudza C, Sorofa W, Chiyaka ET (2012) Assessing the effects of estrogen on the dynamics of breast cancer. Comput Math Methods Med 2012:473572. https://doi.org/10.1155/2012/473572

Nebeling LC, Miraldi F, Shurin SB, Lerner E (1995) Effects of a ketogenic diet on tumor metabolism and nutritional status in pediatric oncology patients: two case reports. J Am College Nutr 14(2):202–208. https://doi.org/10.1080/07315724.1995.10718495

Oke SI, Matadi MB, Xulu SS (2018) Optimal control analysis of a mathematical model for breast cancer. Math Comput Appl 23(2):21. https://doi.org/10.3390/mca23020021

Quirke VM (2017) Tamoxifen from failed contraceptive pill to best-selling breast cancer medicine: a case-study in pharmaceutical innovation. Front Pharmacol 8:620. https://doi.org/10.3389/fphar.2017.00620

Rieger J, Baehr O, Hattingen E, Maurer G, Coy J, Weller M, Steinbach J (2010) The ERGO trial: a pilot study of a ketogenic diet in patients with recurrent glioblastoma. J Clin Oncol 28(15):e12532–e12532

Rieger J, Bähr O, Maurer GD, Hattingen E, Franz K, Brucker D, Walenta S, Kämmerer U, Coy JF, Weller M, Steinbach JP (2014) ERGO: a pilot study of ketogenic diet in recurrent glioblastoma. Int J Oncol 44(6):1843–1852. https://doi.org/10.3892/ijo.2014.2382

Sastre-Garau X, Jouve M, Asselain B, Vincent-Salomon A, Beuzeboc P, Dorval T, Durand JC, Fourquet A, Pouillart P (1996) Infiltrating lobular carcinoma of the breast, clinicopathologic analysis of 975 cases with reference to data on conservative therapy and metastatic patterns. Cancer 77(1):113–120. https://doi.org/10.1002/(SICI)1097-0142(19960101)77:1%3c113::AID-CNCR19%3e3.0.CO;2-8

Siegel RL, Miller KD, Jemal A (2018) Cancer statistics, 2018. CA Cancer J Clin 68(1):7–30. https://doi.org/10.3322/caac.21442

Sung H, Ferlay J, Siegel RL, Laversanne M, Soerjomataram I, Jemal A, Bray F (2021) Global cancer statistics 2020: GLOBOCAN estimates of incidence and mortality worldwide for 36 cancers in 185 countries. CA Cancer J Clin 71(3):209–249. https://doi.org/10.3322/caac.21660

Weber DD, Aminzadeh-Gohari S, Tulipan J, Catalano L, Feichtinger RG, Kofler B (2020) Ketogenic diet in the treatment of cancer—where do we stand? Mol Metab 33:102–121. https://doi.org/10.1016/j.molmet.2019.06.026

Wolff AC, Domchek SM, Davidson NE, Sacchini V, McCormick B (2013) Cancer of the breast. Abeloff's clinical oncology, 5th edn. Elsevier, Amsterdam, pp 1630–1692. https://doi.org/10.1016/B978-1-4557-2865-7.00091-6

World Health Organisation (2023) Breast cancer. https://www.who.int/news-room/fact-sheets/detail/breast-cancer. Accessed 12 Oct 2023

Yousef FB, Yousef A, Abdeljawad T, Kalinli A (2020a) Mathematical modeling of breast cancer in a mixed immune-chemotherapy treatment considering the effect of ketogenic diet. Eur Phys J plus 135(12):1–23. https://doi.org/10.1140/epjp/s13360-020-00991-8

Yousef A, Bozkurt F, Abdeljawad T (2020b) Mathematical modeling of the immune-chemotherapeutic treatment of breast cancer under some control parameters. Adv Differ Equ 2020(1):1–25. https://doi.org/10.1186/s13662-020-03151-5